Article

Triggering Water Exchange Mechanisms via Chelate Architecture. Shielding of Transition Metal Centers by Aminopolycarboxylate Spectator Ligands

Joachim Maigut, Roland Meier, Achim Zahl, and Rudi van Eldik

J. Am. Chem. Soc., **2008**, 130 (44), 14556-14569 • DOI: 10.1021/ja802842q • Publication Date (Web): 08 October 2008

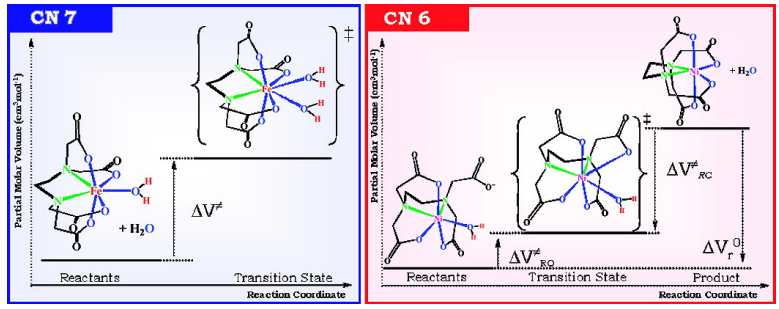

More About This Article

Additional resources and features associated with this article are available within the HTML version:

- Supporting Information
- Access to high resolution figures
- Links to articles and content related to this article
- Copyright permission to reproduce figures and/or text from this article

View the Full Text HTML

J|A|C|S
ARTICLES

Published on Web 10/08/2008

Triggering Water Exchange Mechanisms via Chelate Architecture. Shielding of Transition Metal Centers by Aminopolycarboxylate Spectator Ligands

Joachim Maigut, Roland Meier, Achim Zahl, and Rudi van Eldik*

Inorganic Chemistry, Department of Chemistry and Pharmacy, University of Erlangen-Nürnberg, Egerlandstrasse 1, 91058 Erlangen, Germany

Received April 17, 2008; E-mail: vaneldik@chemie.unierlangen.de

Abstract: Paramagnetic effects on the relaxation rate and shift difference of the ^{17}O nucleus of bulk water enable the study of water exchange mechanisms on transition metal complexes by variable temperature and variable pressure NMR. The water exchange kinetics of $[Mn^{II}(edta)(H_2O)]^{2-}$ (CN 7, hexacoordinated edta) was reinvestigated and complemented by variable pressure NMR data. The results revealed a rapid water exchange reaction for the $[Mn^{II}(edta)(H_2O)]^{2-}$ complex with a rate constant of $k_{ex} = (4.1 \pm 0.4) \times 10^8$ s^{-1} at 298.2 K and ambient pressure. The activation parameters $\Delta H^{\ddagger}$, $\Delta S^{\ddagger}$, and $\Delta V^{\ddagger}$ are 36.6 $\pm$ 0.8 kJ mol^{-1}, +43 $\pm$ 3 J K^{-1} mol^{-1}, and +3.4 $\pm$ 0.2 cm^3 mol^{-1}, which are in line with a dissociatively activated interchange (I_d) mechanism. To analyze the structural influence of the chelate, the investigation was complemented by studies on complexes of the edta-related tmdta (trimethylenediaminetetraacetate) chelate. The kinetic parameters for $[Fe^{II}(tmdta)(H_2O)]^{2-}$ are $k_{ex} = (5.5 \pm 0.5) \times 10^6$ s^{-1} at 298.2 K, $\Delta H^{\ddagger} = 43 \pm 3$ kJ mol^{-1}, $\Delta S^{\ddagger} = +30 \pm 13$ J K^{-1} mol^{-1}, and $\Delta V^{\ddagger} = +15.7 \pm 1.5$ cm^3 mol^{-1}, and those for $[Mn^{II}(tmdta)(H_2O)]^{2-}$ are $k_{ex} = (1.3 \pm 0.1) \times 10^8$ s^{-1} at 298.2 K, $\Delta H^{\ddagger} = 37.2 \pm 0.8$ kJ mol^{-1}, $\Delta S^{\ddagger} = +35 \pm 3$ J K^{-1} mol^{-1}, and $\Delta V^{\ddagger} = +8.7 \pm 0.6$ cm^3 mol^{-1}. The water containing species, $[Fe^{III}(tmdta)(H_2O)]^{-}$ with a fraction of 0.2, is in equilibrium with the water-free hexa-coordinate form, $[Fe^{III}(tmdta)]^{-}$. The kinetic parameters for $[Fe^{III}(tmdta)(H_2O)]^{-}$ are $k_{ex} = (1.9 \pm 0.8) \times 10^7$ s^{-1} at 298.2 K, $\Delta H^{\ddagger} = 42 \pm 3$ kJ mol^{-1}, $\Delta S^{\ddagger} = +36 \pm 10$ J K^{-1} mol^{-1}, and $\Delta V^{\ddagger} = +7.2 \pm 2.7$ cm^3 mol^{-1}. The data for the mentioned tmdta complexes indicate a dissociatively activated exchange mechanism in all cases with a clear relationship between the sterical hindrance that arises from the ligand architecture and mechanistic details of the exchange process for seven-coordinate complexes. The unexpected kinetic and mechanistic behavior of $[Ni^{II}(edta')(H_2O)]^{2-}$ and $[Ni^{II}(tmdta')(H_2O)]^{2-}$ is accounted for in terms of the different coordination number due to the strong preference for an octahedral coordination environment and thus a coordination equilibrium between the water-free, hexadentate $[M(L)]^{n+}$ and the aqua-pentadentate forms $[M(L')(H_2O)]^{n+}$ of the Ni^{II}-edta complex, which was studied in detail by variable temperature and pressure UV−vis experiments. For $[Ni^{II}(edta')(H_2O)]^{2-}$ (CN 6, pentacoordinated edta) a water substitution rate constant of $(2.6 \pm 0.2) \times 10^5$ s^{-1} at 298.2 K and ambient pressure was measured, and the activation parameters $\Delta H^{\ddagger}$, $\Delta S^{\ddagger}$, and $\Delta V^{\ddagger}$ were found to be 34 $\pm$ 1 kJ mol^{-1}, −27 $\pm$ 2 J K^{-1} mol^{-1}, and +1.8 $\pm$ 0.1 cm^3 mol^{-1}, respectively. For $[Ni^{II}(tmdta')(H_2O)]^{2-}$, we found $k = (6.4 \pm 1.4) \times 10^5$ s^{-1} at 298.2 K, $\Delta H^{\ddagger} = 22 \pm 4$ kJ mol^{-1}, and $\Delta S^{\ddagger} = -59 \pm 5$ J K^{-1} mol^{-1}. The process is referred to as a water substitution instead of a water exchange reaction, since these observations refer to the intramolecular displacement of coordinated water by the carboxylate moiety in a ring-closure reaction.

Introduction

The fact that ethylenediaminetetraacetate (edta, Scheme 1) is one of the most produced organic compounds raises critical questions concerning detrimental effects of this compound on the environment. Because of its poor biodegradability and noneffective decomposition in sewage plants, it is ubiquitously distributed in the environment. It can be found in typical concentrations from 10 to 100 nM in groundwater,[1] lake water,[2] and rivers.[3]

Due to its exceptionally high complex formation constants for numerous metal cations, remobilization of cationic sediments, e.g., iron oxides,[4,5] may increase the concentration of dissolved metals in groundwater. The reactivity of these complexes is often determined by the lability of an additionally bound water molecule. The displacement of this solvent molecule is a crucial step in ternary complex formation reactions as well as in many redox processes. For instance, it was found that the oxidation of $Fe^{II}(L)$ complexes by molecular oxygen is

(1) Bergers, P. J. M.; de Groot, A. C. *Water Res.* **1994**, *28*, 639.
(2) Ulrich, M., Ph.D. Dissertation, ETH Zurich, 1991, Diss ETH No. 9632.
(3) Kari, F. G.; Giger, W. *Environ. Sci. Technol.* **1995**, *29*, 2814.
(4) Jardine, P. M.; Jacobs, G. K.; O'Dell, J. D. *Soil Sci. Soc. Am. J.* **1993**, *57*, 954.
(5) Szecsody, J. E.; Zachara, J. M.; Bruckhart, P. L. *Environ. Sci. Technol.* **1994**, *28*, 1706.

10.1021/ja802842q CCC: $40.75

significantly enhanced by the presence of a chelating ligand L.[6] The oxidation of $[Fe^{II}(edta)(H_2O)]^{2-}$ is a typical reaction that requires substitution of water to initially form the dioxygen species $[Fe^{II}(edta)(O_2)]^{2-}$ with subsequent electron transfer leading to $[Fe^{III}(edta)(O_2^-)]^{2-}$ and further reactions as shown below.

$$[Fe^{II}(edta)(H_2O)]^{2-} + O_2 \rightleftharpoons [Fe^{II}(edta)(O_2)]^{2-} + H_2O \quad (1a)$$

$$[Fe^{II}(edta)(O_2)]^{2-} \rightarrow [Fe^{III}(edta)(O_2^-)]^{2-} \quad (1b)$$

$$[Fe^{III}(edta)(O_2^-)]^{2-} + [Fe^{II}(edta)(H_2O)]^{2-} \rightarrow [(edta)Fe^{III}\text{-}(\mu\text{-}O_2^{2-})\text{-}Fe^{III}(edta)]^{4-} + H_2O \quad (1c)$$

$$[(edta)Fe^{III}\text{-}(\mu\text{-}O_2^{2-})\text{-}Fe^{III}(edta)]^{4-} + 2H^+ + 2H_2O \rightarrow 2[Fe^{III}(edta)(H_2O)]^- + H_2O_2 \quad (1d)$$

Hydrogen peroxide is produced in this reaction, which can cause further problems due to its high oxidation potential. For instance, a sequence-specific double-strand cleavage of DNA was observed for the related compounds bis-(Fe^{II}-edta-distamycin) and (Fe^{II}-edta-distamycin).[7] For Fe^{II}-(methidiumpropyl-edta) efficient DNA cleavage with low sequence specificity was found in the presence of molecular oxygen. The observed products are consistent with oxidative degradation of the desoxyribose ring of the DNA backbone, most probably via the formation of hydroxyl radicals.[8] Aside from the remobilization of metal cations from sediments, the complexation by edta and related chelates must be considered in terms of the activation of these metal cations, promoting or enabling further reactions.

However, some of the rare reports on water exchange kinetics of transition metal edta complexes offer incomplete understanding of the reactions of these complexes, since mainly the exchange kinetics at ambient conditions were examined. For instance, studies on $[Ni^{II}(edta')(H_2O)]^{2-}$[9] (CN 6, pentacoordinated edta) and $[Mn^{II}(edta)(H_2O)]^{2-}$[10] (CN 7, hexacoordinated edta) do not allow a detailed assignment of the exchange mechanism since variable pressure experiments were not performed. In general, it can be expected that encapsulation by an aminopolycarboxylate ligand should lead to a pronounced dissociative nature of the exchange reaction due to steric constraints induced by the chelate. The reported temperature dependencies point to this expectation through considerably positive values for the activation entropies, except for $[Ni^{II}(edta')(H_2O)]^{2-}$. Here a value of $\Delta S^{\ddagger} = -29 \pm 8$ J K^{-1} mol^{-1} is more indicative of an associative mechanism. This rather unexpected behavior may arise from the properties of the coordination sphere of the aminopolycarboxylate chelate, which in itself depends on the size and charge of the metal center.

The central metal ions in the studied complexes differ in charge, and especially in d-electron configuration and ionic radii, which will give rise not only to different reaction rates but also to changes in the overall water exchange mechanism. The investigations focus on the water exchange reactions of the Ni^{II}, Fe^{II}, Fe^{III}, and Mn^{II} complexes of both closely related ligands edta and tmdta (= trimethylenediaminetetraacetate, Scheme 1). The latter was chosen to clarify the influence of an elongated diamine ligand backbone on the water-exchange kinetics and the underlying mechanism. To study the water-exchange reaction in case of these labile, paramagnetic complexes, we studied the effect of temperature and pressure on the transverse relaxation rate of the bulk water ^{17}O nucleus.

Scheme 1. Structures of the Hexadentate Aminopolycarboxylate Ligands edta and tmdta

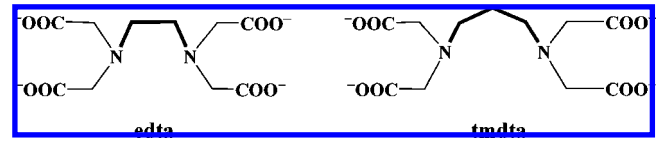

For the discussion and understanding of the individual overall mechanisms, it should be clear which structures the contributing species adopt in aqueous solution. For the Fe^{III}-edta and Fe^{III}-tmdta complexes, it is well established that these can adopt both seven-[11] and six-coordinate[12,13] structures. In solution, predominance of the seven-coordinate, water-containing fraction was in general found.[14,15] The situation is quite similar in the case of Fe^{II}-edta,[16,17] as well as for Mn^{II}-edta[18−20] and Mn^{II}-tmdta.[21]

In the case of Ni^{II}-edta, the situation is more complex. In general, in structures of isolated complexes published for the $[Ni^{II}(edta)]^{2-}$ ion,[22−28] the ligand is bound in a hexadentate way to the Ni^{II} center and the complex anions do not contain coordinated water molecules. There is, however, one report on a series of isomorphous Ni^{II}-edta/Co^{II}-edta structures of the type $Co^{II}_x[Ni^{II}_{2-x}(edta)(H_2O)]\cdot H_2O$ with (x = 2.0, 1.5, 1.0, 0.7).[29] From the structure estimated for $Co^{II}[Co^{II}(edta)(H_2O)]\cdot H_2O$, the conclusion can be drawn that an aqua-pentadentate coordination sphere does exist in $Co^{II}[Ni^{II}(edta')(H_2O)]\cdot H_2O$, which comprises the ring-opened form in aqueous solution. The fraction

(6) Zang, V.; van Eldik, R. *Inorg. Chem.* **1990**, *29*, 1705.
(7) Schultz, P. G.; Dervan, P. B. *J. Am. Chem. Soc.* **1983**, *105*, 7748.
(8) Hertzberg, R. P.; Dervan, P. B. *Biochemistry* **1984**, *23*, 3934.
(9) Grant, M.; Dodgen, H. W.; Hunt, J. P. *Chem. Commun.* **1970**, 1446. (a) Grant, M.; Dodgen, H. W.; Hunt, J. P. *J. Am. Chem. Soc.* **1971**, *93*, 6828.
(10) Zetter, M. S.; Grant, M. W.; Wood, E. J.; Dodgen, H. W.; Hunt, J. P. *Inorg. Chem.* **1972**, *11*, 2701.
(11) Meier, R.; Heinemann, F. W. *Inorg. Chim. Acta* **2002**, *337*, 317.
(12) Novozhilova, N. V.; Polynova, T. N.; Porai-Koshits, M. A.; Pechurova, N. I.; Martynenko, L. I.; Khadi, A. *Zh. Strukt. Khim.* **1973**, *14*, 745.
(13) Meier, R.; Maigut, J.; Kallies, B.; Lehnert, N.; Paulat, F.; Heinemann, F. W.; Zahn, G.; Feth, M. P.; Krautscheid, H.; van Eldik, R. *Chem. Commun.* **2007**, 3960.
(14) Kanamori, K.; Dohniwa, H.; Ukita, N.; Kanesaka, I.; Kawai, K. *Bull. Chem. Soc. Jpn.* **1990**, *63*, 1447.
(15) Sakane, H.; Watanbe, I.; Ono, K.; Ikeda, S.; Kaizaki, S.; Kushi, Y. *Inorg. Chim. Acta* **1990**, *178*, 67.
(16) Mizuta, T.; Wang, J.; Miyoshi, K. *Bull. Chem. Soc. Jpn.* **1993**, *66*, 2547.
(17) Mizuta, T.; Wang, J.; Miyoshi, K. *Inorg. Chim. Acta* **1995**, *230*, 119.
(18) Ananjeva, N. N.; Polynova, T. N.; Porai-Koshits, M. A. *Zh. Strukt. Khim.* **1974**, *15*, 261.
(19) Solans, X.; Gali, S.; Font-Altaba, M.; Oliva, J.; Herrera, J. *Afinidad* **1988**, *45*, 243.
(20) Yi, T.; Gao, S.; Li, B. *Polyhedron* **1998**, *17*, 2243.
(21) Rychlewska, U.; Warżajtisa, B.; Cvetiæ, D.; Radanoviæ, D. D.; Gurešiæc, D. M.; Djuran, M. I. *Polyhedron* **2007**, *26*, 1717.
(22) Sisoeva, T. F.; Agre, V. M.; Trunov, V. K.; Dyatlova, N. M.; Fridman, A. Y.; Barkhanova, N. N. *Zh. Strukt. Khim.* **1981**, *22*, 99.
(23) Agre, V. M.; Sisoeva, T. F.; Trunov, V. K.; Fridman, A. Y.; Barkhanova, N. N. *Zh. Strukt. Khim.* **1981**, *22*, 114.
(24) Agre, V. M.; Sisoeva, T. F.; Trunov, V. K.; Efremov, V. A.; Fridman, Y. A.; Barkhanova, N. N. *Zh. Strukt. Khim.* **1980**, *21*, 110.
(25) Nesterova, Y. M.; Porai-Koshits, M. A. *Koord. Khim.* **1984**, *10*, 129.
(26) Coronado, E.; Drillon, M.; Fuertes, A.; Beltran, D.; Mosset, A.; Galy, J. *J. Am. Chem. Soc.* **1986**, *108*, 900.
(27) Sisoeva, T. F.; Agre, V. M.; Trunov, V. K.; Dyatlova, N. M.; Fridman, A. Y. *Zh. Strukt. Khim.* **1986**, *27*, 108.
(28) Leonteva, M. V.; Fridman, A. Y.; Dyatlova, N. M.; Agre, V. M.; Sysoeva, T. F. *Zh. Neorg. Khim.* **1987**, *32*, 2494.
(29) Pedro Gomez-Romero, P.; Jameson, G. B.; Casan-Pastor, N.; Coronado, E.; Beltran, D. *Inorg. Chem.* **1986**, *25*, 3171.

Scheme 2. Structural Changes that Accompany Equilibrium (7)

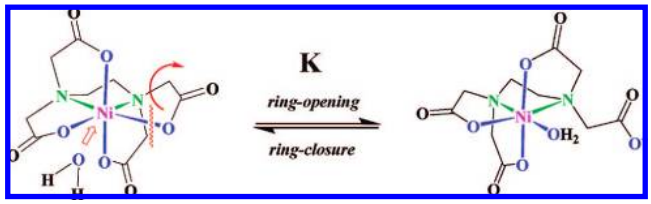

of this form present in aqueous solution is still a matter of discussion as described below.

There are debates in the literature concerning the most suitable "structural" speciation in solutions of Ni^{II}-edta. A number of researchers concluded that all the dissolved material between pH 3 and 10 should be present as $[Ni^{II}(edta)]^{2-}$ with a hexadentate edta and no coordinated water molecule.[30−33] Other workers prefer a view where the main fraction in solution is $[Ni^{II}(edta)]^{2-}$ with a hexadentate edta chelate that equilibrates with a smaller fraction of $[Ni^{II}(edta')(H_2O)]^{2-}$ (aqua-pentadentate form; see Scheme 2), where edta acts as a pentadentate chelate and a water molecule is bound to the Ni^{II} center.[9,34−36] It is our intention to offer a clarification of this query based on new temperature- and pressure-dependent spectrophotometric measurements for the hexadentate ⇌ aqua-pentadentate equilibrium, which allow us to interpret the obtained experimental data (especially the experimental activation volume).

Experimental Section

Materials. The reagents used in this study were all of analytical grade quality, and solutions were prepared in doubly distilled water. The samples for the water exchange measurements were prepared by dissolving the ligands H_4edta (Acros Organics) and H_4tmdta (Acros Organics) in 0.1 M sodium acetate buffer solution (Fisher Chemicals). The pH was measured with a Metrohm 713 pH-Meter using a Metrohm glass electrode (filled with sodium chloride instead of potassium chloride to prevent precipitation of poorly soluble potassium perchlorate) and adjusted to pH = 5.0 with NaOH (Acros Organics). The ionic strength was adjusted with $NaClO_4$ (Merck) to $I = 0.5$ M. The solution was deoxygenated several times under vacuum and saturated with argon before the appropriate amount of $Ni(ClO_4)_2 \cdot 6H_2O$ (Fluka), $FeSO_4 \cdot 7H_2O$ (Acros Organics), $FeCl_3 \cdot 6H_2O$ (Acros Organics), or $Mn(ClO_4)_2 \cdot 6H_2O$ (Acros Organics) was added. To study the exchange kinetics, the complex solution was enriched with the NMR active ^{17}O isotope by adding argon saturated $H_2{}^{17}O$ (10%, Deutero) using syringe techniques to give a total enrichment of 1% ^{17}O in the measured samples.

For the preparation of $Ca[Ni(edta)] \cdot 4H_2O$, 2.92 g (0.01 mol) of H_4edta were suspended in 20 mL of doubly distilled water and the mixture was heated to 80 °C on a stirring plate. After addition of 1.48 g (0.02 mol) of $Ca(OH)_2$, heating on the stirring plate was continued until a clear solution was formed. Now, 3.66 g (0.01 mol) of $[Ni(H_2O)_6] \cdot 2ClO_4$ were added and a clear blue solution resulted in due course. After cooling to room temperature, 40 mL of ethanol were added and the solution was placed in a refrigerator. After 2 days, bright shining blue crystals were formed. These were separated by filtration and air-dried. Yield: 3.0 g, 65.4%. Anal. Calcd for $C_{10}H_{20}Ca_2N_2NiO_{12}$ (MW = 459.0 g/mol): C, 26.16; H, 4.39; N, 6.10. Found: C, 26.10; H, 4.50; N, 6.05.

^{17}O NMR Measurements. ^{17}O NMR spectra were recorded on a Bruker AVANCE DRX 400WB spectrometer equipped with a spectrospin superconducting widebore magnet operating at a resonance frequency of 54.24 MHz at a magnetic induction of 9.4 T. The measurements at atmospheric pressure were performed with a commercial 5 mm Bruker broadband probe thermostatted with a Bruker B-VT 3000 variable temperature unit. To avoid susceptibility corrections of the measured data in the determination of the shift of the ^{17}O resonance, the sample was sealed in a 4 mm sphere fitted inside a standard NMR tube. The samples with and without the paramagnetic compound were concentrically surrounded by an external deuterated standard (toluene) for locking. The chemical shifts as well as the line width at half-height of the signal were determined by a deconvolution procedure on the real part of the Fourier transformed spectra with a Lorentzian shape function in the data analysis module of Bruker Topspin 1.3 software. For variable pressure measurements a homemade thermostatted high pressure probe[37] was used. The sample was placed in a standard 5 mm NMR tube cut to a length of 50 mm and closed with a moveable macor piston. The pressure was transmitted to the sample by pressurizing the surrounding perfluorated hydrocarbon (hexafluoropropyleneoxide, Hostinert 175, Hoechst). The applied pressure in the probe was monitored by a VDO gauge with an accuracy of ±1%. Temperature was controlled by circulating thermostatted water (Colora thermostat WK 16) to ±0.1 K of the desired temperature and monitored before each measurement with an internal Pt-resistance thermometer with an accuracy of ±0.2 K.

UV−vis Measurements. Sample solutions for pH-, pressure-, and temperature-dependent UV−vis measurements were prepared from standard solutions that contained precise amounts of $Ca[Ni(edta)] \cdot 4H_2O$. pH-dependent spectrophotometric titrations were carried out with a Varian CARY 5 UV−visible spectrophotometer fitted with a thermostatted sample holder. All measurements were carried out at 25.0 ± 0.2 °C in 1 M $NaClO_4$. Pressure-dependent UV−vis spectra were measured with a homemade high pressure unit connected to a Shimadzu UV-2101 spectrophotometer.[38] UV−vis spectral measurements in dependence of temperature were made on a CARY 5 spectrophotometer coupled to a commercial VARIAN temperature control unit.

Results and Discussion

Water Exchange Reactions. The exchange rates of solvent molecules between the bulk and the coordination site of paramagnetic complexes are accessible by studying the apparent paramagnetic influence on the relaxation rates and on the resonance shift of the ^{17}O nucleus for bulk water molecules as a function of temperature. The exchange rates of the bound water molecules were determined by the line-broadening technique developed by Swift and Connick.[39,40] Their approach makes use of the relationship between the reduced transverse relaxation rate ($1/T_{2r}$) and the mean lifetime of the coordinated solvent (τ_m) (eq 2). The full treatment of transverse relaxation (eq 3) needs to consider contributions from the transverse relaxation time of coordinated water in the inner-sphere of the complex in the absence of chemical exchange (T_{2m}), the difference in resonance frequency of bulk solvent and solvent in the first coordination sphere ($\Delta\omega_m$), and the above-mentioned mean lifetime of coordinated solvent (τ_m). The exchange rate constant between coordinated and bulk solvent, k_{ex}, can accordingly be

(30) Bhat, T. R.; Krishnamurty, M. *J. Inorg. Nucl. Chem.* **1963**, *25*, 1147.
(31) Bhat, T. R.; Radhamma, D.; Shankar, J. *J. Inorg. Nucl. Chem.* **1965**, *27*, 2641.
(32) Matwiyoff, N. A.; Strouse, C. E.; Morgan, L. O. *J. Am. Chem. Soc.* **1970**, *92*, 5222.
(33) Felmy, A. R.; Qafoku, O. *J. Solution Chem.* **2004**, *33*, 1161.
(34) Higginson, W. C. E.; Samuel, B. *J. Chem. Soc. A.* **1970**, 15796.
(35) Erickson, L. E.; Young, D. C.; Ho, F. F.-L.; Watkins, S. R.; Terrill, J. B.; Reilley, C. N. *Inorg. Chem.* **1971**, *10*, 441.
(36) Evilia, R. F. *Inorg. Chem.* **1985**, *24*, 2076.
(37) Zahl, A.; Neubrand, A.; Aygen, S.; van Eldik, R. *Rev. Sci. Instrum.* **1994**, *65*, 882.
(38) Spitzer, M.; Gartig, F.; van Eldik, R. *Rev. Sci. Instrum.* **1988**, *59*, 2092.
(39) Swift, T. J.; Connick, R. E. *J. Chem. Phys.* **1962**, *37*, 307.
(40) Swift, T. J.; Connick, R. E. *J. Chem. Phys.* **1964**, *41*, 2553.

expressed as the reciprocal residence time of the bound solvent molecule $k_{ex} = 1/\tau_m$. T_{2os} represents an outer-sphere contribution to T_{2r} that arises from long-range interactions of the paramagnetic unpaired electrons of the metal complex with water molecules outside the first coordination sphere.

$$\pi \cdot \frac{1}{P_m}(\Delta\nu_{obs} - \Delta\nu_{solvent}) = \frac{1}{T_{2r}} = \frac{1}{\tau_m}\left\{\frac{T_{2m}^{-2} + (T_{2m}\tau_m)^{-1} + \Delta\omega_m^2}{(T_{2m}^{-1} + \tau_m^{-1})^2 + \Delta\omega_m^2}\right\} + \frac{1}{T_{2os}} \quad (2)$$

$$\frac{1}{T_{2r}} = \frac{1}{\tau_m}\left\{\frac{T_{2m}^{-2} + (T_{2m}\tau_m)^{-1} + \Delta\omega_m^2}{(T_{2m}^{-1} + \tau_m^{-1})^2 + \Delta\omega_m^2}\right\} \quad (2a)$$

$$\frac{1}{T_{2r}} = \frac{1}{\tau_m}\left\{\frac{\Delta\omega_m^2}{\tau_m^{-2} + \Delta\omega_m^2}\right\} \quad (2b)$$

$$\Delta\omega_r = \frac{1}{P_m}(\omega_{obs} - \omega_0) = \frac{\Delta\omega_m}{(1 + \tau_m T_{2m}^{-1})^2 + \tau_m^2\Delta\omega_m^2} + \Delta\omega_{os} \quad (3)$$

The determination of $1/T_{2r}$ requires the measurement of the full line widths at half-height of the ^{17}O NMR signal of the bulk solvent in the presence ($\Delta\nu_{obs}$) and absence ($\Delta\nu_{solvent}$) of the paramagnetic compound, normalized to the mole fraction of bound water (P_m). The line-broadening experiments were performed at concentrations which assured a reasonable broadening compared to the aqueous reference ($\Delta\nu_{obs} - \Delta\nu_{solvent} >$ 20 Hz).

In the case of a significant resonance shift, additional shift-analysis experiments were performed in a spherical NMR tube. Here, the signal shift was never determined in a simple peak picking procedure. Instead, the ^{17}O resonances were fitted at each adjusted temperature with a Lorentzian function to give the accurate signal position. The reduced chemical shift difference, $\Delta\omega_r$, was calculated from the observed chemical shifts of the sample solution, ω_{obs}, and the aqueous reference in the absence of the paramagnetic compound, ω_0, and normalized by the mole fraction of bound water P_m. The relationship between $\Delta\omega_r$ and T_{2m}, chemical shift ($\Delta\omega_m$, $\Delta\omega_{os}$), and residence time (τ_m) is given by eq 3.

The separation of the contributing factors in eqs 2−3 is achieved by measuring their temperature dependencies. These measurements are, in principle, restricted to a rather small kinetic window between the boiling and freezing points of water. Depending on the exchange kinetics of the studied systems, these possible contributions are not all observable in the available temperature range. A contribution of $1/T_{2os}$ to the reduced transverse relaxation rate that would be clearly visible by a changeover to a positive slope at low temperatures (very slow exchange domain, I) was not observed for any of the investigated systems. The absence of this contribution justifies the application of eq 2 in a reduced form (eq 2a), where outer-sphere contributions to relaxation are ignored. At elevated temperatures, some compounds show contributions from $1/T_{2m}$. In that case, an exponential Arrhenius-type temperature dependence was applied in the treatment of the bound water relaxation rate $1/T_{2m}$ given by eq 4.

$$\frac{1}{T_{2m}} = \frac{1}{T_{2m}^0}\exp\left\{\frac{E_m}{RT}\right\} \quad (4)$$

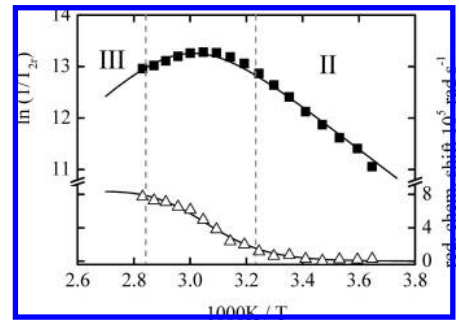

Figure 1. Temperature dependence of the reduced transverse relaxation rate, $1/T_{2r}$ (■, refers to left axis) and of the reduced chemical shift difference, $\Delta\omega_r$ for the ^{17}O NMR resonance (Δ, refers to right axis) for $[Ni^{II}(edta')(H_2O)]^{2-}$ (Table S1-1/2, Supporting Information). The solid lines result from the simultaneous least-squares fit of the measured data for both experiments and deliver the activation parameters ($\Delta H^{\ddagger}$ and $\Delta S^{\ddagger}$) given in Table 1.

Equation 2b refers to the treatment of the exchange kinetics in the absence of an observable T_{2m} contribution. The dependence of the exchange rate constant (k_{ex}) on temperature variation can be derived from the Eyring equation (eq 5). Here the reciprocal residence time, or k_{ex}, depends on the activation parameters for the water exchange process, viz. the activation enthalpy, $\Delta H^{\ddagger}$, and activation entropy, $\Delta S^{\ddagger}$.

$$k_{ex} = \frac{1}{\tau_m} = \left(\frac{k_B T}{h}\right)\exp\left\{\left(\frac{\Delta S^{\ddagger}}{R}\right) - \left(\frac{\Delta H^{\ddagger}}{RT}\right)\right\} \quad (5)$$

For $\Delta\omega_m$, a reciprocal temperature dependence was applied. The hyperfine coupling constant (A/h) serves as a proportionality factor and defines the relationship between temperature variation and chemical shift of the bound water molecule. Equation 6 gives the mathematical treatment that describes the temperature dependence of $\Delta\omega_m$ involving (A/h) as a proportionality constant.

$$\Delta\omega_m = \frac{2\pi \cdot g_L \mu_B S(S+1)B}{3k_B T}\left(\frac{A}{h}\right) \quad (6)$$

As already outlined in the Introduction, kinetic and mechanistic studies concerning the water substitution reaction of $[Ni^{II}(edta')(H_2O)]^{2-}$ require the consideration of the equilibrium between the ring-closed hexadentate and the ring-opened aqua-pentadentate species (reaction 7) in solution as it is depicted in Scheme 2.

$$\underset{hexadentate\ edta}{[Ni^{II}(edta)]^{2-}} + H_2O \rightleftharpoons \underset{pentadentate\ edta}{[Ni^{II}(edta')(H_2O)]^{2-}} \quad (7)$$

The fraction of the water containing species was calculated at each temperature from the available data for the temperature dependence of the combined aquation/ring-opening equilibrium constant K (ref 36, P_m values given in Table S1-1/2, Supporting Information). For $[Ni^{II}(edta')(H_2O)]^{2-}$ the temperature dependence of the reduced transverse relaxation rate, $1/T_{2r}$ (Figure 1, upper curve) and of the reduced chemical shift difference, $\Delta\omega_r$ (Figure 1, lower curve), was studied in two independent experiments. A standard NMR tube was applied for the determination of $1/T_{2r}$, whereas the measurement of $\Delta\omega_r$ required a spherical distribution of the sample in the magnetic center to avoid susceptibility corrections. The inflection point in the variable temperature measurement of $\Delta\omega_r$ was found at the same temperature, where the maximum is located in the $\ln(1/T_{2r})$ vs $1/T$ plot. A changeover to the fast exchange region

Table 1. Rate and Activation Parameters for Water Substitution of $M^{II/III}$-edta Complexes Derived from the Variable Temperature Measurements of the Line-Broadening and Shift Difference ($\Delta H^{\ddagger}$ and $\Delta S^{\ddagger}$) and the Pressure Dependence of the Water Substitution Rate Constant k ($\Delta V^{\ddagger}$)[a]

	10^{-5} k_{298K}, s^{-1}	(A/h), Hz	$\Delta H^{\ddagger}$, kJ mol^{-1}	$\Delta S^{\ddagger}$, J K^{-1} mol^{-1}	$\Delta V^{\ddagger}$, cm^3 mol^{-1}
$[Ni^{II}(edta')(H_2O)]^{2-}$[a]	2.6 ± 0.2	$(2.9 \pm 0.3) \times 10^7$	34 ± 1	−27 ± 2	+1.8 ± 0.1
$[Ni^{II}(edta')(H_2O)]^{2-}$[b]	3.1 ± 2.8[c]	$(2.6 \pm 0.2) \times 10^7$	33 ± 5	−29 ± 12	–
$[Fe^{II}(edta)(H_2O)]^{2-}$[d]	27 ± 1	1.0×10^7	43.2 ± 0.5	+23 ± 2	+8.6 ± 0.4
$[Fe^{III}(edta)(H_2O)]^{-}$[e]	720	6.5×10^7[f]	24.3 ± 0.7	−13 ± 2	+1.9 ± 0.3
$[Mn^{II}(edta)(H_2O)]^{2-}$	4100 ± 400	$(6.4 \pm 0.2) \times 10^6$	36.6 ± 0.8	+43 ± 3	+3.4 ± 0.2
$[Mn^{II}(edta)(H_2O)]^{2-}$[g]	4300 ± 300	$(6.04 \pm 0.15) \times 10^6$	32.1 ± 0.4	+28 ± 1	–

[a] Calculated with $P_m(T)$, considering the temperature dependence of the isomeric equilibrium constant with the literature data from ref 36 (Table S1-1/2, Supporting Information). [b] Reference 9. [c] calculated from the reported activation parameters in ref 9. [d] Reference 44. [e] Reference 45. [f] Calculated from the reported A value. [g] Reference 10.

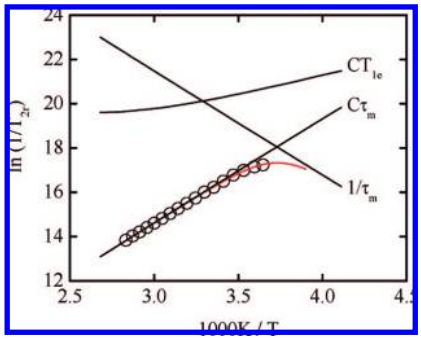

Figure 2. Temperature dependence of the reduced transverse relaxation rate, $1/T_{2r}$ of $[Mn^{II}(edta)(H_2O)]^{2-}$(O), and of the three contributions from $1/\tau_m$, $C\tau_m$, and CT_{1e}. The least-squares fit to the data (red) with eq 2d and the literature values for τ_v, E_v, and Δ[10], yielded the kinetic and NMR parameters given in Tables 1 and 2b.

(II → III) is evident in both techniques, which correspondingly show the proposed changeover in the dominating contributions.

From the obtained value for the hyperfine coupling constant ($A/h = 2.9 \times 10^7$ Hz), which is very similar to $A/h = 2.6 \times 10^7$ Hz reported by Hunt[9] and also close to values reported for $[Ni^{II}(H_2O)_6]^{2+}$ ($A/h = (2.0 - 2.4) \times 10^7$ Hz),[41−43] the thermodynamic parameters and the K value given in ref 36 appear reasonable. The obtained activation parameters confirm the literature values but could be fixed with more precision than those given in ref 9 (see Table 1). A comparison with the calculated kinetic data, neglecting any temperature dependence for K (Table S1-3 and Figure S1-3, Supporting Information), shows that the activation parameters are rather insensitive to temperature dependent changes of K in the accessible temperature window. The calculated values for k_{ex} (the exchange rate constant) from the obtained values of the activation enthalpy and entropy along the two different evaluation procedures are identical within experimental error (Figure S1−3, Supporting Information).

In the case of $[Mn^{II}(edta)(H_2O)]^{2-}$, the temperature dependence for $1/T_{2r}$ (Figure 2) revealed a changeover to the fast exchange regime (III) at lower temperatures as compared to the $[Ni^{II}(edta')(H_2O)]^{2-}$ system (Figure 1). Furthermore, the relative long T_{1e} for Mn(II) complexes causes T_{2m} contributions to dominate in eq 2a with negligible contributions from $\Delta\omega_m$.[46,47]

$$\frac{1}{T_{2r}} = \frac{1}{\tau_m + T_{2m}} \tag{2c}$$

In the reduced eq 2c, the transverse relaxation is dominated by the scalar relaxation mechanism, $1/T_{2c}$ (eq 8), with the longitudinal electronic relaxation term being the determining factor in transverse relaxation.

$$\frac{1}{T_{2m}} \cong \frac{1}{T_{2sc}} = \frac{1}{3}S(S+1)\left(\frac{A}{\hbar}\right)^2\left(\tau_{s1} + \frac{\tau_{s2}}{1+\tau_{s2}^2\omega_s^2}\right) \tag{8}$$

$$\frac{1}{\tau_{si}} = \frac{1}{\tau_m} + \frac{1}{T_{ie}} \tag{8a}$$

The electron spin relaxation rates are mainly governed by a transient zero-field splitting mechanism (ZFS) described by eq 9.[48]

$$\frac{1}{T_{1e}} = \frac{32}{25}\Delta^2\left(\frac{\tau_v}{1+\tau_v^2\omega_s^2} + \frac{4\tau_v}{1+4\tau_v^2\omega_s^2}\right) \tag{9}$$

$$\tau_v = \tau_v^{298}\exp\left\{\frac{E_v}{R}\left(\frac{1}{T} - \frac{1}{298.2}\right)\right\} \tag{9a}$$

The combination of eqs 2c, 8, and 9 gives the adequate description of the relevant contributions to T_{2r} for Mn^{II} species, eq 2d.

$$\frac{1}{T_{2r}} = 1\Big/\left(\tau_m + \frac{1}{C}\left(\frac{1}{\tau_m} + \frac{1}{T_{1e}}\right)\right) \tag{2d}$$

with

$$C = \frac{4\pi^2}{3}S(S+1)\left(\frac{A}{h}\right)^2 \tag{9c}$$

For $[Mn^{II}(edta)(H_2O)]^{2-}$, the fit of the relaxation data with eq 2d was carried out with the literature values for τ_v, E_v and Δ[10] ($T_{1e} = 1.27 \times 10^{-7}$ s). The optimization of T_{1e} in the fitting procedure yielded $T_{1e} = 1.42 \times 10^{-7}$ s, which agrees well with the above given literature value (Figure S2-1). The assumption of a temperature independent T_{1e} contribution does not influence the kinetic parameters within the experimental accuracy (Table 2). The reason for the observation that the activation parameters are rather insensitive to the different data treatments comes from the very small contribution from T_{1e} to the overall relaxation process. The system is in the fast exchange regime with a very high water exchange rate, so that the maximum contribution from electronic relaxation is ~3.5% at 273 K; at the temperature

(41) Neely, J. W.; Connick, R. E. *J. Am. Chem. Soc.* **1972**, *94*, 3519.
(42) Bechtold, D. B.; Liu, G.; Dodgen, H. W.; Hunt, J. P. *J. Phys. Chem.* **1978**, *82*, 333.
(43) Ducommun, Y.; Earl, W. L.; Merbach, A. E. *Inorg. Chem.* **1979**, *18*, 2754.
(44) Maigut, J.; Meier, R.; Zahl, A.; van Eldik, R. *Inorg. Chem.* **2007**, *46*, 5361.
(45) Schneppensieper, T.; Seibig, S.; Zahl, A.; Tregloan, P.; van Eldik, R. *Inorg. Chem.* **2001**, *40*, 3670.
(46) Zetter, M. S.; Dodgen, H. W.; Hunt, J. P. *Biochemistry* **1973**, *12*, 778.
(47) Oakes, J.; Smith, E. G. *J. Chem. Soc., Faraday Trans. 1* **1983**, *79*, 543.
(48) McLachlan, A. D. *Proc. R. Soc. London, Ser. A* **1964**, *280*, 271.

Table 2. Kinetic and NMR Parameters Derived in the Variable Temperature ^{17}O NMR Relaxation Measurements of $[Mn^{II}(edta)(H_2O)]^{2-}$

parameters	fit results[a]	fit results[b]
χ^2/DoF	0.000 54	0.000 46
R^2	0.999 66	0.999 69
C	$(5.18 \pm 2.59) \times 10^{15}$	$(4.73 \pm 0.3) \times 10^{15}$
T_{1e} [s]	$(1.42 \pm 0.3) \times 10^{-7}$	1.27×10^{-7}
$\Delta H^{\ddagger}$ [kJ mol^{-1}]	36.7 ± 0.8	36.6 ± 0.8
$\Delta S^{\ddagger}$ [J K^{-1} mol^{-1}]	44 ± 6	43 ± 3
$\tau_{v,\,298K}$ [s]		1.42×10^{-12}[c]
Δ [rad s^{-1}]		3.64×10^{9}[c]
E_v [kJ mol^{-1}]		15.0[c]

[a] Asuming a temperature independent T_{1e} contribution. [b] Considering the temperature dependence of T_{1e} by fitting the data with a temperature dependent τ_v value. [c] Fom ref 10.

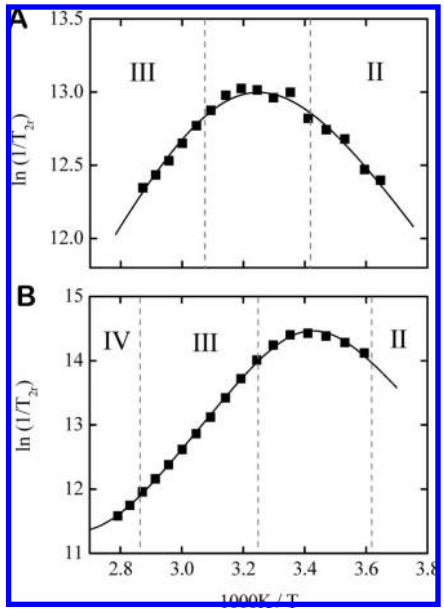

Figure 3. (A) Temperature dependence of the reduced transverse relaxation rate, $1/T_{2r}$, of (■) $[Ni^{II}(tmdta')(H_2O)]^{2-}$. (B) Temperature dependence of the reduced transverse relaxation rate, $1/T_{2r}$, of 20 mM (■) $[Fe^{II}(tmdta)(H_2O)]^{2-}$. The obtained activation parameters $\Delta H^{\ddagger}$ and $\Delta S^{\ddagger}$ are given in Table 3.

of the variable pressure experiment (293.2 K) the contribution is only 2.2%. Figure 2 shows the plot of the measured transverse relaxation rate versus reciprocal temperature together with the three contributions from $1/\tau_m$, $C\tau_m$, and CT_{1e} to T_{2r}.

The obtained activation parameters and the value for the hyperfine coupling constant are in agreement with literature data.[10] The coordinated water molecule was found to be strongly labilized with respect to the fully aquated complex with an exchange rate constant of $(4.1 \pm 0.4) \times 10^8$ s^{-1} at 298.2 K. The significantly positive value for the activation entropy for $[Mn^{II}(edta)(H_2O)]^{2-}$, viz. $\Delta S^{\ddagger} = +43 \pm 3$ J K^{-1} mol^{-1}, is indicative of a dissociatively activated interchange mechanism.

To extend the understanding of the interdependences between the shielding properties of chelate ligands (L) and the exchange kinetics of the water molecule in the cavity of the metal complex $[M(L)(H_2O)]^{n-}$, we investigated the reactivity of analogues transition metal tmdta complexes. In the case of $[Ni^{II}(tmdta')(H_2O)]^{2-}$ (Figure 3A), the slow- (II) and fast-exchange domain (III) were accessible in the applied temperature range of the relaxation experiment. Because of the fact that no details on the equilibrium reaction (7) for the $[Ni^{II}(tmdta)]^{2-}/[Ni^{II}(tmdta')(H_2O)]^{2-}$ system are reported so far, we deduced the amount of the water containing fraction in a fitting procedure by application of the literature value for the hyperfine coupling constant for the $Ni^{II}-O$ interaction of the $[Ni^{II}(edta')(H_2O)]^{2-}$ system, $(A/h) = 2.6 \times 10^7$ Hz (Table S3-1 and Figure S3-1, Supporting Information).[9] The obtained value of $P_m = 1.23 \times 10^{-4}$ reveals a very small fraction of ~3% $[Ni^{II}(tmdta')(H_2O)]^{2-}$ in solution. This finding accounts for the necessity of a high total concentration of Ni^{II}-tmdta (250 mM) to measure significant line width changes during the temperature variation study. Although temperature effects on K are expected to be too small to significantly affect the activation parameters in the temperature range of the NMR experiments (see for instance the $[Ni^{II}(edta)]^{2-}/[Ni^{II}(edta')(H_2O)]^{2-}$ system), we evaluated the possible impact by including a temperature dependence for the equilibrium constant K between the ring-closed form, $[Ni^{II}(tmdta)]^{2-}$ (RC), and the ring-opened form, $[Ni^{II}(tmdta')(H_2O)]^{2-}$ (RO) (eqs 10 and 11). Despite the small fraction of the water containing species and ΔH°_r as an additional free parameter in the fit, the result for the equilibrium constant is in reasonable agreement with the determined value given above, with a fraction of the ring-opened species of $f_{RO} = 0.034$. Indeed, the activation parameters are rather insensitive to such a treatment and show only slight deviations from the treatment neglecting any temperature dependence of K (Figure S3-2, Supporting Information). The activation parameters in Table 3 are given with larger error limits to account for the overall error from both data treatment procedures.

$$K^T_{RC\rightarrow RO} = K^{298}_{RC\rightarrow RO} \exp\left\{-\frac{\Delta H^{\circ}_r}{R}\left(\frac{1}{T} - \frac{1}{298.2}\right)\right\} \qquad (10)$$

$$P_m = \left\{\frac{K^T_{6\rightarrow 7}}{(K^T_{6\rightarrow 7} + 1)}\right\} c[\text{Complex}]/55.55 \qquad (11)$$

The $[Fe^{II}(tmdta)(H_2O)]^{2-}$ (Figure 3B) and $[Fe^{III}(tmdta)(H_2O)]^{-}$ (Figure 4) data were fitted with an additional contribution from T_{2m} (eq 2a), since in both cases, region (IV) is accessible at higher temperatures. In the case of $[Fe^{III}(tmdta)(H_2O)]^{-}$, a preliminary fit to the $\ln(1/T_{2p})$ data with a typical (A/h) value for the $Fe^{III}-O$ interaction (6×10^7 Hz)[44,45] revealed a minor fraction ($f = 0.2$) of the water containing, aqua-hexadentate species (CN 7) in equilibrium with the water-free hexadentate (CN 6) form, $[Fe^{III}(tmdta)]^{-}$ (Table S6-1 and Figure S6-1, Supporting Information). Thus, to account for the smaller concentration of $[Fe^{III}(tmdta)(H_2O)]^{-}$, relaxation and shift data were analyzed with a P_m value of 7.2×10^{-5} (Table S6-2/3, Supporting Information), an additional treatment considering the temperature variation of P_m according to eq 11 does not affect the activation parameters significantly. The obtained values for the activation parameters, $\Delta H^{\ddagger} = 42 \pm 3$ kJ mol^{-1} and $\Delta S^{\ddagger} = 32 \pm 10$ J K^{-1} mol^{-1}, and for $K = 0.29 \pm 0.03$ and thus a fraction of the aqua-hexadentate form (CN 7) of $f = 0.2$, agree very well with the treatment neglecting any temperature variation, but with the disadvantage of a lower accuracy (Figure S6-2, Supporting Information). To account for this uncertainty, we report the activation parameters in Table 3 with increased error limits.

The mathematical treatment of the transverse relaxation of $[Mn^{II}(tmdta)(H_2O)]^{2-}$ (Figure 5) again requires the consideration of the large T_{2m} contribution for Mn^{II} systems. Thus, the data fitting was performed by the simplified Swift−Connick eq 2d. The obtained value for the electronic relaxation time $T_{1e} = 1.51 \times 10^{-7}$ s is comparable to that of $[Mn^{II}(edta)(H_2O)]^{2-}$. The

Table 3. Rate and Activation Parameters for Water Substitution of $M^{II/III}$-tmdta Complexes Derived from the Variable Temperature Measurements of the Line-Broadening and Shift Difference ($\Delta H^{\ddagger}$ and $\Delta S^{\ddagger}$) and the Pressure Dependence of the Water Substitution Rate Constant k ($\Delta V^{\ddagger}$)[a]

	10^{-5} k_{298K}, s^{-1}	(A/h), Hz	$\Delta H^{\ddagger}$, kJ mol^{-1}	$\Delta S^{\ddagger}$, J K^{-1} mol^{-1}	$\Delta V^{\ddagger}$, cm^3 mol^{-1}
$[Ni^{II}(tmdta')(H_2O)]^{2-}$[a]	6.4 ± 1.4	2.6×10^7	22 ± 4	−59 ± 5	+5.0 ± 0.6[c]
$[Fe^{II}(tmdta)(H_2O)]^{2-}$	55 ± 5	1.7×10^7	43 ± 3	+30 ± 13	+15.7 ± 1.5
$[Fe^{III}(tmdta)(H_2O)]^{-}$[b]	190 ± 80	6.0×10^7	42 ± 3	+36 ± 10	+7.2 ± 2.7[d]
$[Mn^{II}(tmdta)(H_2O)]^{2-}$	1320 ± 100	1.2×10^7	37.2 ± 0.8	+35 ± 3	+8.7 ± 0.6

[a] Refers to a fraction of the water containing species $f = 0.028$ and $P_m = 1.23 \times 10^{-4}$. [b] Refers to a fraction of the water containing species $f = 0.2$ and $P_m = 7.2 \times 10^{-5}$. [c] With $\Delta V^{\circ}_r = -7.9$ cm^3 mol^{-1}. [d] The value is estimated by applying ΔV°_r ranging from −2.5 to −7.5 cm^3 mol^{-1}.

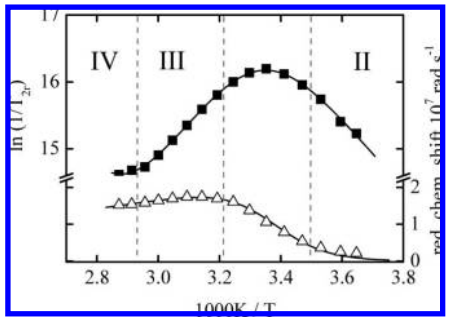

Figure 4. Temperature dependence of the reduced transverse relaxation rate, $1/T_{2r}$ (■, refers to left axis), and of the reduced chemical shift difference, $\Delta\omega_r$, of the ^{17}O NMR resonance (Δ, refers to right axis) of $[Fe^{III}(tmdta)(H_2O)]^-$ ($P_m = 7.2 \times 10^{-5}$). The solid lines result from a simultaneous least-squares fit to the measured data from both experiments and yielded the activation parameters $\Delta H^{\ddagger} = 42 \pm 2$ kJ mol^{-1} and $\Delta S^{\ddagger} = 36 \pm 6$ J mol^{-1} K^{-1} (the values given in Table 3 account for the error limits due to the temperature dependence of P_m).

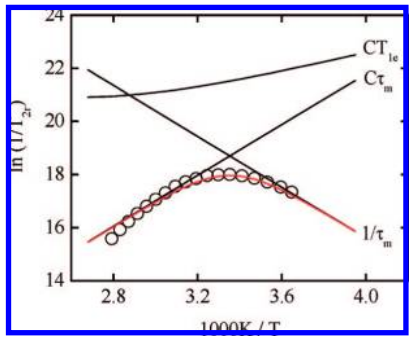

Figure 5. Temperature dependence of the reduced transverse relaxation rate, $1/T_{2r}$, of $[Mn^{II}(tmdta)(H_2O)]^{2-}$ (○) and of the three contributions from $1/\tau_m$, $C\tau_m$, and CT_{1e} to T_{2r}. The least-squares fit to the data (red) with eq 2d yielded the kinetic and NMR parameters given in Tables 3 and 4.

contribution from CT_{1e} to the overall transverse relaxation is negligibly small (max. 3% at 303.2 K). Thus, the activation parameters are found largely insensitive in both data treatments, with first a variable and second a fixed T_{1e} parameter (Tables 3 and 4).

A comparison of the kinetic data for water exchange reactions obtained so far (Table 5), reveals an increase in k_{ex} along the series $[Fe^{II}(edta)(H_2O)]^{2-}$ < $[Fe^{III}(edta)(H_2O)]^{-}$ < $[Mn^{II}(edta)(H_2O)]^{2-}$ (see Table 5). This observed trend can be rationalized as a consequence of the variation of charge and d-electron occupancy. The divalent species $[M^{II}(edta)(H_2O)]^{2-}$ with M = Fe and Mn give rise to a lowering of the water exchange rate with increasing occupancy of the d orbitals. This is exactly what is expected for a transition metal solvent exchange process

Table 4. Kinetic and NMR Parameters Derived from the Variable Temperature ^{17}O NMR Relaxation Measurements of $[Mn^{II}(tmdta)(H_2O)]^{2-}$

parameters	fit results[a]	fit results[b]
χ^2/DoF	0.010 79	0.009 65
R^2	0.965 56	0.972 24
C	$(1.9 \pm 0.6) \times 10^{16}$	$(1.75 \pm 0.5) \times 10^{16}$
T_{1e} [s]	1.51×10^{-7}	1.27×10^{-7}
$\Delta H^{\ddagger}$ [kJ mol^{-1}]	37.1 ± 1.7	37.2 ± 0.8
$\Delta S^{\ddagger}$ [J K^{-1} mol^{-1}]	36 ± 6	35 ± 3
$\tau_{v,\,298K}$ [s]	–	1.42×10^{-12}[c]
Δ [rad s^{-1}]	–	3.64×10^{9}[c]
E_v [kJ mol^{-1}]	–	15.0[c]

[a] assuming a temperature independent T_{1e} contribution. [b] considering the temperature dependence of T_{1e} by fitting the data with a temperature dependent τ_v value. [c] from ref 10.

Table 5. Rate Constants and Activation Volumes for Water Exchange at Seven-Coordinate $[M^{II/III}(L)(H_2O)]^{2-/-}$ Complexes of M = Fe^{II}, Fe^{III}, and Mn^{II} with L = edta and tmdta[a]

complex	$k_{ex,298}$, s^{-1}	$\Delta V^{\ddagger}$, cm^3 mol^{-1}	ref
$[Ni^{II}(H_2O)_6]^{2+}$	3.15×10^4	+7.2	51
$[Fe^{II}(H_2O)_6]^{2+}$	$(4.4 \pm 0.3) \times 10^6$	+3.8	51
$[Fe^{III}(H_2O)_6]^{3+}$	1.6×10^2	−5.4	52/53
$[Mn^{II}(H_2O)_6]^{2+}$	2.1×10^7	−5.4	51
$[Fe^{II}(edta)(H_2O)]^{2-}$	$(2.7 \pm 0.1) \times 10^6$	+8.6 ± 0.4	44
$[Fe^{III}(edta)(H_2O)]^{-}$	7.2×10^7	+1.9 ± 0.3	46
$[Mn^{II}(edta)(H_2O)]^{2-}$	$(3.2 \pm 0.1) \times 10^8$	+3.4 ± 0.2	this work
$[Fe^{II}(tmdta)(H_2O)]^{2-}$	$(5.5 \pm 0.5) \times 10^6$	+15.7 ± 1.5	this work
$[Fe^{III}(tmdta)(H_2O)]^{-}$	$(1.9 \pm 0.8) \times 10^7$	+7.2 ± 2.7	this work
$[Mn^{II}(tmdta)(H_2O)]^{2-}$	$(1.3 \pm 0.1) \times 10^8$	+8.7 ± 0.6	this work

[a] For comparison the values of the corresponding fully aquated complexes $[M^{II/III}(H_2O)_6]^{2+/3+}$ are also shown.

triggered by ligand field effects and shows the same trend as found for $[M(H_2O)_6]^{2+}$ with M = Ni, Fe and Mn.[51] Although Fe^{III} has the same d-electron configuration as Mn^{II}, the water exchange reaction is significantly slower. Here a second effect, viz. the higher charge density is responsible for the observed trend. The complexation of the Fe^{III} cation by the aminopolycarboxylate ligand leads to donation of electron density to the metal center through combined σ- and π-donating properties of the edta donor atoms. The water exchange process is enhanced tremendously, with a resulting reactivity that lies between that of $[Fe^{II}(edta)(H_2O)]^{2-}$ and $[Mn^{II}(edta)(H_2O)]^{2-}$. Despite the smaller formal charge, $[Fe^{II}(edta)(H_2O)]^{2-}$ shows a slower water exchange reaction than its trivalent analogue because of the higher ligand-field activation energy (LFAE). This is similar to the classical examples of $[V(H_2O)_6]^{3+}$ (t_{2g}^2) and $[V(H_2O)_6]^{2+}$ (t_{2g}^3), where the water exchange of the trivalent

(49) Ducommun, Y.; Zbinden, D.; Merbach, A. E. *Helv. Chim. Acta* **1982**, *65*, 1385.
(50) Hugi, A. D.; Helm, L.; Merbach, A. E. *Helv. Chim. Acta* **1985**, *68*, 508.
(51) Ducommun, Y.; Newman, K. E.; Merbach, A. E. *Inorg. Chem.* **1980**, *19*, 3696.
(52) Grant, M.; Jordan, R. B. *Inorg. Chem.* **1981**, *20*, 55.
(53) Swaddle, T. W.; Merbach, A. E. *Inorg. Chem.* **1981**, *20*, 4212.

species is about six times faster than for the divalent ion.[49,50] The complexes of Ni^{II}, viz. $[Ni^{II}(L')(H_2O)]^{2-}$ with L= edta and tmdta, are characterized by the slowest water substitution reaction for each series. Here, the electronic configuration ($t_{2g}^6e_g^2$) and thus the strong preference for octahedral coordination lead to a totally different mechanism for the water displacement. The bound water in the ring-opened form $[Ni^{II}(L')(H_2O)]^{2-}$ is displaced by the entering carboxylate group leading to the formation of the ring-closed form (see below).

Interesting is an evaluation of the effect of complexation by the edta ligand on k_{ex}. For Fe^{III} and Mn^{II}, chelation leads to an enhanced water exchange reaction compared to the fully aquated species. This is not surprising, since both have a high-spin d^5 configuration with no appreciable angular dependence on ligand field stabilization. Despite the coordination sphere formed by the chelate ligand, conformational changes required during the water substitution process are easily feasible in d^5 systems since no contribution to the activation energy is apparent. The electron-donating properties of the aminopolycarboxylate chelate enhance water exchange on the higher charged trivalent iron species by several orders of magnitude, whereas, in the case of the already fast exchanging divalent Mn^{II} aqua species, a moderate enhancement is found. For Fe^{II}, a meaningful contribution to the activation energy makes the water exchange slower as compared to the fully aquated species. However, in the case of Ni^{II} a somewhat different situation is apparent. Water exchange is faster for the chelated species despite an expected stabilization through its d^8 electronic configuration. A possible explanation for this unexpected behavior as a result of chelation can point to differences in the underlying exchange mechanism and requires further mechanistic considerations. To substantiate mechanistic interpretations that are so far solely based on the sign and the value of the activation entropy, we performed high pressure NMR experiments. Such studies on the pressure dependence of the exchange rate constant have in recent years led to the mechanistic clarification of numerous solvent exchange processes.[54−59] Pressure dependent measurements are best performed in the slow exchange domain (II) because of an existing direct proportionality, viz. $1/T_{2r} \approx k_{ex}$. However, from the above shown temperature dependencies, it is obvious that region (II) is not accessible in all cases. Therefore, the variable pressure experiment was performed in a linear segment close to the maximum of the plot of $\ln(1/T_{2r})$ vs $1/T$ in the fast exchange region (III). In this exchange domain eq 12 approximates the observed transverse relaxation.

$$\frac{1}{T_{2r}} \cong \tau_m \Delta\omega_m^2 \tag{12}$$

Because of the reciprocal dependence of $1/T_{2r}$ and k_{ex} in the fast exchange domain the observed increase in the transverse relaxation rate with pressure is caused by a decrease in the water exchange rate. The pressure dependence of the exchange rate constant at a fixed temperature T is given by eq 13.[60−62] The activation volume, $\Delta V^{\ddagger}$, is defined as the difference between the partial molar volumes of the transition and reactant states.

$$\left(\frac{\partial \ln(k)}{\partial p}\right)_T = -\frac{\Delta V^{\ddagger}}{RT} \tag{13}$$

$$\ln k_p = \ln k_0 - \frac{\Delta V_0^{\ddagger} P}{RT} + \frac{\Delta\beta^{\ddagger} P^2}{2RT} \tag{14}$$

Equation 14 is an approximate solution for the differential eq 13 in the case of a pressure dependent $\Delta V^{\ddagger}$. Here, k_p and k_0 represent the rate constants at pressure P and atmospheric pressure, respectively. $\Delta V_0^{\ddagger}$ is the activation volume at zero pressure and temperature T, and $\Delta\beta^{\ddagger}$ is the compressibility coefficient of activation. The exchange rate constants at different pressures, k_p, were obtained as solutions either to the full or to the reduced Swift−Connick equations (eqs 2a and 2b,c). For a mechanistic interpretation of variable pressure experiments on solvent exchange reactions, it has to be considered that the principle of microscopic reversibility requires symmetrical reaction coordinates for the forward and reverse reaction as reactant and product are equivalent. Consequently, the entering and leaving solvent molecules have substantial bonding to the metal center in an associatively activated solvent interchange (I_a) process. In the case of a dissociatively activated interchange (I_d) process, weak bond formation with the entering solvent molecule is accompanied by weak bonding of the leaving solvent molecule required by symmetry.

The exchange rate constants k_p were determined at pressures ranging from 2 to 150 MPa, first from low to high pressure, and then from high to low pressure. In this way the reproducibility of the line widths as a function of pressure was verified and the arithmetic average was used for the determination of the activation volume. For $[Mn^{II}(edta)(H_2O)]^{2-}$ the pressure dependence of the kinetic and electronic terms in eq 2d was considered (see Table S8 and Figure S8, Supporting Information). Using limiting values of ± 2 cm^3 mol^{-1} for the electronic relaxation does not change the value of the activation volume or the value of the exchange rate constant, which is due to the above-mentioned very minor influence from the CT_{1e} term at the applied temperature (~2.2%). The activation volume, $\Delta V^{\ddagger} = +3.4 \pm 0.2$ cm^3 mol^{-1}, is slightly more positive than that for the isoelectronic $[Fe^{III}(edta)(H_2O)]^-$ system (Figure 6, ×).[45] From the sign and the value of $\Delta V^{\ddagger}$ the mechanism is reliably identified as a dissociatively activated interchange (I_d) process, which is the expected mechanism for the exchange of a water molecule in seven-coordinate complexes with a considerable shielded metal center (see below). A comparison of the rate constants derived from the variable temperature, $k_{ex} = (3.2 \pm 0.4) \times 10^8$ s^{-1} (293.2 K), and from the variable pressure experiment, $k_0 = (3.3 \pm 0.03) \times 10^8$ s^{-1}, shows excellent agreement.

In contrast to the activation volumes for the fully aquated species that show a changeover in mechanism from I_d to I_a along the series Ni^{II}, Fe^{II}, Fe^{III}, and Mn^{II}, which is paralleled by an increase in ionic radius, the chelated species show a somewhat different trend (see Table 5). The encapsulation of the metal cations by the edta ligand leads to considerably more positive

(54) Helm, L.; Merbach, A. E. *Chem. Rev.* **2005**, *105*, 1923.
(55) DeVito, D.; Weber, J.; Merbach, A. E. *Inorg. Chem.* **2004**, *43*, 858.
(56) Thompson, M. K.; Botta, M.; Nicolle, G.; Helm, L.; Aime, S.; Merbach, A. E.; Raymond, K. N. *J. Am. Chem. Soc.* **2003**, *125*, 14274.
(57) Grundler, P. V.; Helm, L.; Alberto, R.; Merbach, A. E. *Inorg. Chem.* **2006**, *45*, 10378.
(58) Houston, J. R.; Richens, D. T.; Casey, W. H. *Inorg. Chem.* **2006**, *45*, 7962.
(59) Swaddle, T. W.; Rosenqvist, J.; Yu, P.; Bylaska, E.; Phillips, B. L.; Casey, W. H. *Science* **2005**, *308*, 1450.
(60) Whalley, E. *Adv. Phys. Org. Chem.* **1964**, *2*, 93.
(61) Eckert, C. A. *Annu. Rev. Phys. Chem.* **1972**, *23*, 239.
(62) Stranks, D. R. *Pure Appl. Chem.* **1974**, *38*, 303.

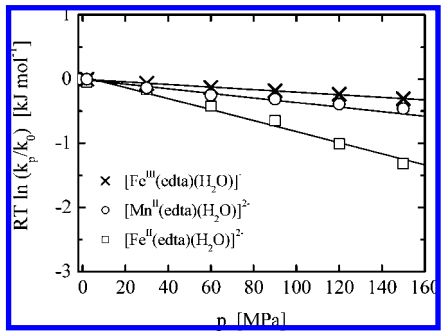

Figure 6. Pressure dependence of the water exchange rate constant derived from the variable pressure relaxation studies of $[Mn^{II}(edta)(H_2O)]^{2-}$ (○ at 293.2 K). For comparison, the reported data for $[Fe^{III}(edta)(H_2O)]^{-}$ (×) and $[Fe^{II}(edta)(H_2O)]^{2-}$ (□) are also plotted.[44,45] The activation volumes from a linear fit of the data and the exchange rate constants extrapolated to atmospheric pressure, k_0, are given in Table 1 and in the text.

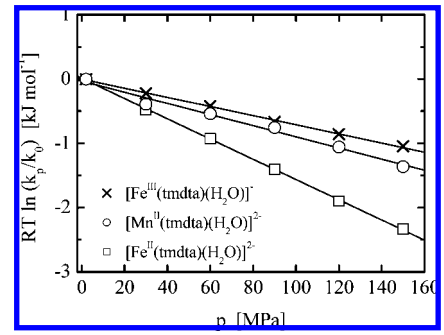

Figure 7. Pressure dependence of the water exchange rate constants derived from the variable pressure relaxation studies of $[Mn^{II}(tmdta)(H_2O)]^{2-}$ (○ at 333.2 K), $[Fe^{III}(tmdta)(H_2O)]^{-}$ (× at 318.2 K), and $[Fe^{II}(tmdta)(H_2O)]^{2-}$ (□ at 318.2 K). The activation volumes from a linear fit of the data and the exchange rate constants extrapolated to atmospheric pressure, k_0, are given in Table 3 and in the text.

activation volumes (except for Ni^{II} see below), because of the shielding by the spectator ligand. In the case of Mn^{II} and Fe^{III} this leads to a complete changeover in mechanism. This is a result of the steric constraints formed around the metal center. These seven-coordinate species can undergo substitution only by a more or less extensive elongated bond of the water molecule in the seventh coordination site to allow the entering of a water molecule from the second coordination sphere(see Scheme 4 A). Consequently, it can be expected that the exchange of edta for a ligand with an elongated backbone, viz. tmdta, will increase the shielding of the metal center with the necessity of a more pronounced dissociative character of the water substitution reaction. Thus, we studied the pressure dependence of the water exchange reactions for a corresponding series of transition metal tmdta complexes (see Figure 7). In the case of $[Fe^{II}(tmdta)(H_2O)]^{2-}$, a linear segment was exclusively accessible in the fast exchange domain (III) and the pressure dependence was carried out at a temperature of 318.2 K (Table S9 B). The obtained values and the linear fit yielded $\Delta V^{\ddagger} = +15.7 \pm 1.5$ cm^3 mol^{-1} and $k_0 = (1.6 \pm 0.2) \times 10^7$ s^{-1} (cf. $k_{ex} = (1.8 \pm 0.2) \times 10^7$ s^{-1} at 318.2 K). The temperature dependence of water exchange on $[Mn^{II}(tmdta)(H_2O)]^{2-}$ revealed incomplete access to the linear part of the slow exchange domain. The variable pressure experiment was therefore performed at 333.2 K. The data treatment included consideration of the impact of pressure variation on the electronic relaxation similar to that for the above-mentioned $[Mn^{II}(edta)(H_2O)]^{2-}$ complex (Table S9 D and Figure S9 D, Supporting Information). Due to the very small contribution from the CT_{1e} term to the overall relaxation at 333.2 K ($\sim$ 1.6%), the values for $\Delta V^{\ddagger}$ and k_{ex} do not significantly change in the different data treatments. The activation volume of $\Delta V^{\ddagger} = +8.7 \pm 0.6$ cm^3 mol^{-1} clearly supports the dissociative character of the interchange process. The obtained exchange rate constant $k_0 = (7.2 \pm 0.1) \times 10^8$ s^{-1} fits well to the value from the temperature dependence study, viz. $k_{ex} = (7.4 \pm 0.2) \times 10^8$ s^{-1} (at 333.2 K). For $[Fe^{III}(tmdta)(H_2O)]^{-}$, the variable pressure NMR data need to be analyzed by considering the effect of pressure on the aforementioned CN 7/CN 6 equilibrium for the species $[Fe^{III}(tmdta)(H_2O)]^{-}$ and $[Fe^{III}(tmdta)]^{-}$, since significant amounts of the water-free, hexa-coordinate species are present in aqueous solution. Due to the lack of experimental data for the pressure dependent species distribution, we are restricted to an estimation of the activation volume. Ascribing a pressure dependence of P_m with a reasonable value of $\Delta V^{\circ}_r = -5$ cm^3 mol^{-1}, along with upper and lower limits for ΔV°_r of -7.5 and -2.5 cm^3 mol^{-1}, resulted in an activation volume for the water exchange reaction of $\Delta V^{\ddagger} = +7.2 \pm 2.7$ cm^3 mol^{-1} (Table S9 C and Figure S9 C, Supporting Information), which is expected for such a system and close to $\Delta V^{\ddagger} = +8.7 \pm 0.6$ cm^3 mol^{-1} for the isoelectronic $[Mn^{II}(tmdta)(H_2O)]^{2-}$. The comparison with $\Delta V^{\ddagger} = +1.9 \pm 0.3$ cm^3 mol^{-1} for $[Fe^{III}(edta)(H_2O)]^{-}$ and $\Delta V^{\ddagger} = +3.4 \pm 0.2$ cm^3 mol^{-1} for $[Mn^{II}(edta)(H_2O)]^{2-}$ reveals a rather proportional increase in $\Delta V^{\ddagger}$ on going from the edta to the tmdta complexes with the same $\Delta(\Delta V^{\ddagger})$ value of +5.3 cm^3 mol^{-1} for the isoelectronic Fe^{III} and Mn^{II} complexes. Obviously, the ligands give rise to a comparable gradual change in $\Delta V^{\ddagger}$, so that the numerical increase in this case can be reliably related to the smaller cavity size of tmdta as compared to edta.[63] Thus, the degree of $M-OH_2$ bond elongation to reach a proper $M-OH_2$ approach of the incoming water molecule is significantly larger in the case of tmdta as compared to edta complexes. It is furthermore remarkable that the gradual change of the dissociative character (expressed as $\Delta V^{\ddagger}$) along the sequence $Mn^{II} < Fe^{III} < Fe^{II}$ is the same for the edta and tmdta complexes with the a comparable difference $\Delta(\Delta V^{\ddagger})$ between the tmdta and edta series.

In contrast to the seven-coordinate complexes discussed so far, expressed by the general formulas $[M^{II/III}(L)(H_2O)]^{2-/-}$, the water containing species of the nickel complexes is an aqua-pentadentate species with a noncoordinated carboxylate group, $[Ni^{II}(L')(H_2O)]^{2-}$, that equilibrates with the water free, hexadentate species $[Ni^{II}(L)]^{2-}$ (see reaction 7 and Scheme 2). The preference for six-coordination could be related to the d^8 electron configuration of Ni^{II} and thus a significant LFSE effect. It has also been mentioned that Ni^{II} complexes with edta-type ligands show less angular strain than related 3d M^{II} complexes.[64] The average twist angle ϕ, the ratio s/h, and the angle θ have been estimated for the dianion $[Ni(edta)]^{2-}$ (edta as hexadentate ligand) as found in $Ca[Ni^{II}(edta)]\cdot 4H_2O$[25] as well as for the protonated monoanion in $Li[Ni^{II}(Hedta)(H_2O]\cdot H_2O$[65] (edta as pentadentate ligand) along the lines given by Brown and Stiefel.[66] One can clearly recognize by comparing the changes

(63) Maigut, J.; Meier, R.; Zahl, A.; van Eldik, R. *Inorg. Chem.* **2008**, *47*, 5702.
(64) Yamamoto, T.; Mikata, K.; Miyoshi, K.; Yoneda, H. *Inorg. Chim. Acta* **1988**, *150*, 237.
(65) Polynova, T. N.; Filippova, T. V.; Porai-Koshits, M. A. *Koord. Khim.* **1986**, *12*, 273.
(66) Brown, G. F.; Stiefel, E. I. *Inorg. Chem.* **1973**, *12*, 2140.
(67) Porai-Koshits; M. A.; Nesterova, Ya. M.; Polynova, T. N.; Turk de Garcia Banus, D. *Koord. Khim.* **1975**, *1*, 682.

Scheme 3. Structural Changes That Accompany Equilibrium (15)

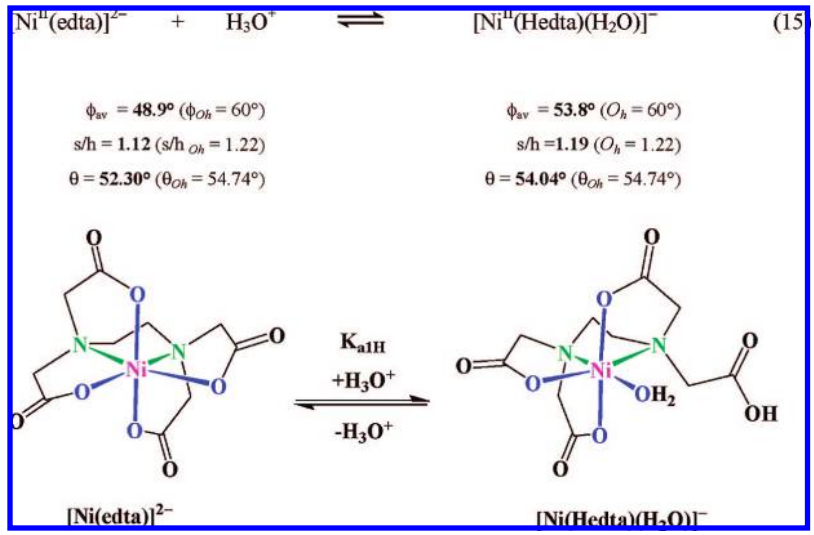

in the structural features upon ring-opening (ϕ_{av} increases from 48.9° to 53.8°, and also the *s*/*h* ratio as well as the angle θ gain more pronounced octahedral character) that the degree of distortion is considerably reduced. One can safely conclude that the changes noticed for the structures that we regard as models for the proton assisted ring-opening reaction (15) are also valid for ring opening driven by the addition of water (reaction 7) as shown in Scheme 2, such that the generation of a considerable fraction of the dianion $[Ni^{II}(edta')(H_2O)]^{2-}$ with an aqua-pentadentate coordination sphere instead of a seven-coordinate species is caused by the strong adherence of the Ni^{II} solution species to an octahedral ligand field. Indeed, kinetic studies by Grant et al. revealed significant amounts of an aqua-edta species present in solution.[9] They suggested the presence of a six-coordinate species with one unprotonated, dechelated acetate arm, $[Ni^{II}(edta')(H_2O)]^{2-}$, at pH 6−7 and an analogous structure at pH 2, with a protonated, dechelated arm, $[Ni^{II}(Hedta)(H_2O)]^-$. The predomination of a ring-opened species at low pH is reasonable in light of the reported crystal structures for the protonated complexes of the type $[Ni^{II}(Hedta)(H_2O)]^-$ [65,67,68] (cf. Scheme 2). In studies by Higginson et al.,[34] it was suggested that 25 ± 2% of the total concentration of Ni^{II}-edta is present in the form of an aqua-pentadentate fraction at neutral pH. The structural speciation of the $[Ni(edta)]^{2-}/[Ni^{II}(edta')(H_2O)]^{2-}$ system in solution was studied in detail by Evilia et al.[36,69,70] using ^1H and ^{13}C NMR. Based on the dependence of the in-plane carboxylate shifts on pH and temperature, an equilibrium between hexadentate and aqua-pentadentate species (reaction 7) was assigned to the resonance pattern. These carboxylate groups were found to be involved in a rapid (lifetime <3 ms) coordinated ⇌ uncoordinated equilibrium, which indicated that at equilibrium (ambient temperature) ~32% of the total concentration of Ni^{II}-edta is present as $[Ni^{II}(edta')(H_2O)]^{2-}$ (K = 0.54 at 298.2 K).

To gain further information on the equilibrium between aqua-pentadentate and hexadentate forms of Ni^{II}-edta, we performed systematic pH, temperature, and pressure dependent UV−vis studies on solutions of Ni^{II}-edta. Spectrophotometric techniques are very suitable for such investigations, since it was already described in the mid-1960s by Bhat and Krishnamurthy[30,31] that one of the spectral consequences on going from the left to the right in reaction (7) is an increase in the molar absorbance of the $^3A_{2g} \rightarrow {}^3T_{1g}(P)$ transition at ~380 nm[30,31] in the spectrum of the product species.

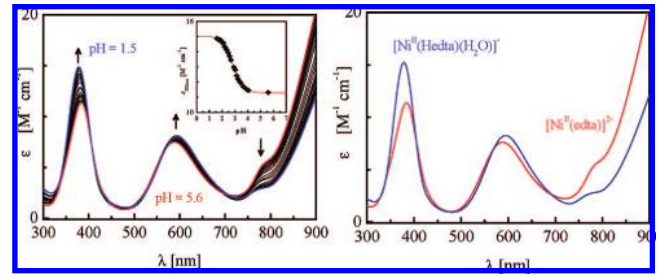

Figure 8. (Left) Spectrophotometric titration of a 0.02 M solution of Ni^{II}-edta (1 M $NaClO_4$, 25 °C) from pH 5.6 to 1.5 monitored between 300 and 900 nm. The inset shows the pH-dependence of the molar absorbance at 380 nm. (Right) Limiting spectra of the species $[Ni^{II}(edta)]^{2-}$ and $[Ni^{II}(Hedta)(H_2O)]^-$ as calculated by SPECFIT, with $pK_{a1H} = 2.74 \pm 0.03$.

An adequate data treatment thus requires the consideration of the structural features that accompany equilibrium (7) to account for temperature and pressure effects on K. An appropriate access to the discussed equilibrium reaction is found in the proton assisted ring-opening reaction (15) shown in Scheme 3. Thus, in Figure 8 we present such spectra for a special case of reaction (7), viz. the reaction with H_3O^+ in reaction (15). In the absence of detailed structural studies, it was already concluded by the earlier workers[30,31] that this type of absorbance increase should be related to the opening of a glycinate chelate ring as a result of the introduction of the ternary ligand at the Ni^{II} center.

$$[Ni^{II}(edta)]^{2-} + H_3O^+ \rightleftharpoons [Ni^{II}(Hedta)(H_2O)]^- \qquad (15)$$

The spectral changes during variable temperature UV−vis experiments (cf. Figure 9) support the thermodynamic parameters ($\Delta H = -14.2$ kJ mol^{-1}, $\Delta S = -58.5$ J K^{-1} mol^{-1}) for the hexadentate pentadentate equilibrium reported by Evilia et al.,[36] where it was shown that the formation of the ring-opened species is exothermic. Correspondingly, we observed an in-

(68) Smith, G. S.; Hoard, J. L. *J. Am. Chem. Soc.* **1959**, *81*, 556.
(69) Everhart, D. S.; Evilia, R. F. *Inorg. Chem.* **1975**, *14*, 2755.
(70) Robert, J. M.; Evilia, R. F. *Inorg. Chem.* **1987**, *26*, 2857.

creased formation of aqua-pentadentate species on lowering the temperature.

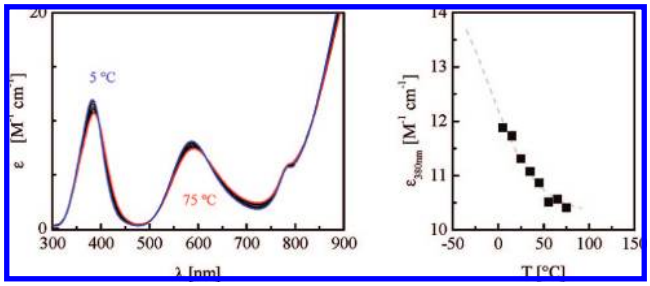

Figure 9. (Left) Temperature dependent spectra of the $[Ni^{II}(edta)]^{2-}$/$[Ni^{II}(edta')(H_2O)]^{2-}$ system ($[Ni^{II}\text{-edta}]_{Total}$ = 0.02 M, 1 M $NaClO_4$, pH 5.6) in the range between 5 and 75 °C. (Right) Temperature dependence of the molar absorbance at 380 nm obtained from the spectra shown on the left side.

However, it is clear that a limiting ϵ_{RC} value for the ring-closed species can only be roughly estimated from the ϵ_{380nm} vs temperature plot due to the limited temperature range of the UV−vis experiment (see Figure 9, right). This is understandable, since the temperature dependent species distribution from the thermodynamic parameters given above still reveals a fraction of 0.2 ring-opened $[Ni^{II}(edta')(H_2O)]^{2-}$ species at 75 °C (cf. Table in Figure 10). Thus, the limiting value was determined from the plot of ϵ_{380nm} and the fraction of the ring-closed f_{RC} at temperatures from 5 to 75 °C. The quality of this extrapolation can be seen from a comparison of the obtained value for ϵ_{RO} = 15.394 M^{-1} cm^{-1} with that of the pH titration (Figure 8), and from the calculated equilibrium constants $K = (\epsilon_{obs} - \epsilon_{RC})/(\epsilon_{RO} - \epsilon_{obs})$ with the observed molar absorbance at 380 nm (ϵ_{obs}) from the pH titration ϵ_{pH} = 11.298 M^{-1} cm^{-1} (at pH 5.6), the variable temperature experiment ϵ = 11.313 M^{-1} cm^{-1} (at 298.2 K, see Figure 10), and the variable pressure experiment ϵ = 11.17 M^{-1} cm^{-1} (at 50 bar, see Table S7−1), yielding K values of 0.52, 0.53, and 0.48, respectively, which is in excellent agreement with the literature value 0.54 (at 298.2 K) reported by Evilia et al.[36] With these limiting values for ϵ_{RC} and ϵ_{RO} for the equilibrating species $[Ni^{II}(edta)]^{2-}$ and $[Ni^{II}(edta')(H_2O)]^{2-}$, respectively, the pressure dependent species distribution and thus the pressure dependence of K can be studied by high pressure UV−vis measurements. The observed spectral changes of the $[Ni^{II}(edta)]^{2-}$/$[Ni^{II}(edta')(H_2O)]^{2-}$ system in the range 5 to 200 MPa are shown in Figure 11 together with the calculated values for the equilibrium constant at each pressure (Table S7-1, Supporting Information).

The observed spectral changes in Figure 11 support the suggested formation of the ring-opened, aqua-pentadentate form on increasing pressure and formation of the hexadentate form on increasing temperature (Figure 9). Equilibrium (7) is shifted to the right on increasing pressure as a result of the coordination of a water molecule and ring opening of an acetate arm of the edta chelate that is accompanied by a significant charge creation. Both of these processes are expected to cause a volume collapse, which accounts for the negative reaction volume and shift in equilibrium (7) to the right as a function of pressure.

From the observed pressure dependence of the isomeric equilibrium constant K (Figure 11 and Table S7-1, Supporting Information) a reaction volume of −7.9 ± 0.2 cm^3 mol^{-1} for equilibrium (7) was calculated. A similar equilibrium for $[Co^{III}(edta)]^-$ was reported to be accompanied by a volume change of −9.5 ± 0.4 cm^3 mol^{-1}.[71] The strong preference for the octahedral coordination geometry is manifested by the observation of the above-mentioned coordination equilibrium between hexadentate ⇌ aqua-pentadentate species with a ring-opened carboxylate group in solution, and thus the significant pressure dependence of the isomeric equilibrium needs to be considered for any mechanistic interpretation that is based on variable pressure experiments.

With the known pressure dependent distribution of the species $[Ni^{II}(edta)]^{2-}$/$[Ni^{II}(edta')(H_2O)]^{2-}$, the P_m values for the data treatment of the variable pressure ^{17}O NMR measurements are accessible (Table S7-2, Supporting Information). The rate of the departure of the coordinated water molecule for the ring-opened species, $[Ni^{II}(edta')(H_2O)]^{2-}$, was found to decrease with increasing pressure (Figure 12, left). For this experimentally determined activation volume, $\Delta V^{\ddagger}$ = +1.8 ± 0.1 cm^3 mol^{-1}, a suitable mechanistic interpretation is required. Here, the NMR observations can be related to either a coordinated/bulk water-exchange process or the substitution of the bound water by the free carboxylate during a ring-closure reaction. The first mechanism seems virtually impossible, due to the obtained value of the activation volume. A water exchange reaction for $[Ni^{II}(edta')(H_2O)]^{2-}$ can be expected to be characterized by a strongly dissociative character due to the preference for octahedral coordination. This is clearly seen from the reported activation volume for $[Ni^{II}(H_2O)_6]^{2+}$, $\Delta V^{\ddagger}$ = +7.2 cm^3 mol^{-1} (Table 6).[51] The second proposed mechanism, a ring-closure process, consists of three components that can contribute to the observed pressure dependence, viz. the dissociation of the water molecule, the coordination of the $-COO^-$ group and the decrease in electrostriction resulting from charge neutralization. In contrast to the simple water exchange process, the combination of these contributions can account for the observed small positive $\Delta V^{\ddagger}$ value, since positive contributions from the first and last contribution together with a pronounced negative volume effect due to carboxylate binding can be expected. This mechanistic proposal is supported not only by the unusual largely negative activation entropies of the $[Ni^{II}(L')(H_2O)]^{2-}$ species but also more decisively by the observation that the water substitution rate constant agrees with the rate of ring opening of the edta chelate reported by Evilia et al.[36,72] As a result, the observed kinetics do not reflect the exchange of a water molecule as discussed above for the seven-coordinate species but are related to a ring-closure reaction of the aqua-pentadentate form. Consequently, the activation volume for the ring-opening process in equilibrium (7) is obtained from $\Delta V^{\circ}_r = \Delta V^{\ddagger}_{RC} - \Delta V^{\ddagger}_{RO}$ and leads to a value of −6.1 cm^3 mol^{-1}. The aquation of the hexa-coordinate species $[Ni^{II}(edta)]^{2-}$ is necessarily connected with a considerable dissociation of a bound carboxylate arm of the chelate ligand. The observed characteristic activation volumes for an associatively activated interchange (I_a) process are absolutely in line with the proposed I_a concerted water-binding/carboxylate-dissociation process (Scheme 4B).

A corresponding analysis of the relaxation data in the variable pressure study of the analogues $[Ni^{II}(tmdta)]^{2-}$/$[Ni^{II}(tmdta')(H_2O)]^{2-}$ system is restricted by an unfavorable equilibrium composition, which leads to insufficiently small spectral changes in the course of variable temperature and pressure UV−vis experiments and prevents a detailed analysis of the analogous equilibrium reaction (7). Thus, a reliable mechanistic assignment

(71) Yoshitani, K. *Bull. Chem. Soc. Jpn.* **1994**, *67*, 2115.

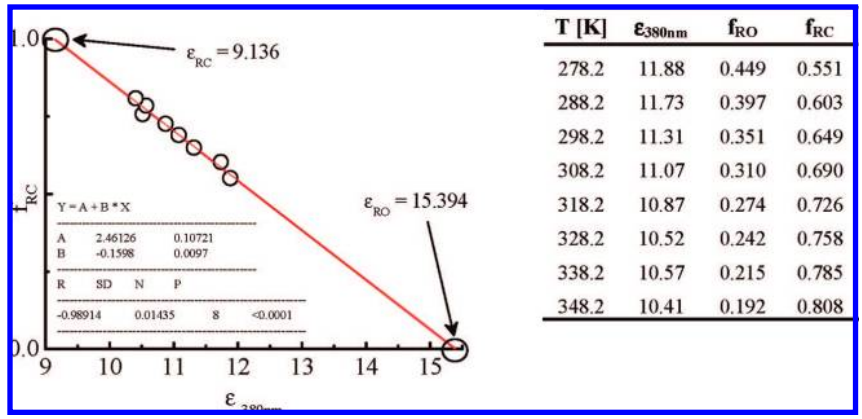

T [K]	ε_{380nm}	f_{RO}	f_{RC}
278.2	11.88	0.449	0.551
288.2	11.73	0.397	0.603
298.2	11.31	0.351	0.649
308.2	11.07	0.310	0.690
318.2	10.87	0.274	0.726
328.2	10.52	0.242	0.758
338.2	10.57	0.215	0.785
348.2	10.41	0.192	0.808

Figure 10. (Left) A plot of ϵ_{380nm} vs the fraction of ring-closed $[Ni^{II}(edta)]^{2-}$ yielded the limiting values for ϵ_{RC} and ϵ_{RO} in good agreement with ϵ_{RO} from the pH titration (Figure 8). (Right) Tabulation of ϵ_{380nm} values from temperature dependent UV−vis experiments and the fraction of the ring-opened (f_{RO}) and ring-closed forms (f_{RC}) calculated from the thermodynamic parameters for K given by Evilia et al.[36]

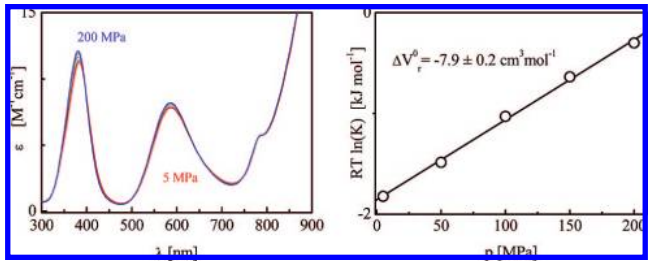

Figure 11. (Left) Pressure dependent spectra of the $[Ni^{II}(edta)]^{2-}$/$[Ni^{II}(edta')(H_2O)]^{2-}$ system ($[Ni^{II}\text{-edta}]_{Total}$ = 0.02 M, 1 M $NaClO_4$, 25 °C, pH 5.6) in the range 5 to 200 MPa. (Right) Pressure dependence of the equilibrium constant $K = (\epsilon_{380nm} - \epsilon_{RC})/(\epsilon_{RO} - \epsilon_{380nm})$ for the hexadentate ⇌ aqua-pentadentate equilibrium (7) from the measured molar absorbances at 380 nm (ϵ_{380nm}), ϵ_{RC} = 9.136 M^{-1} cm^{-1} and ϵ_{RO} = 15.39 M^{-1} cm^{-1} (Table S7-1, Supporting Information).

for the water substitution reaction of $[Ni^{II}(tmdta')(H_2O)]^{2-}$ is not possible. However, if we assume a comparable pressure dependence for the $[Ni^{II}(L)]^{2-}/[Ni^{II}(L')(H_2O)]^{2-}$ equilibria for L = edta and tmdta, this enables a fairly good estimation of the activation volume for the ring-closure reaction of $[Ni^{II}(tmdta')(H_2O)]^{2-}$. In Figure 12 the variable pressure data are shown (○) that were analyzed by considering the pressure dependence of P_m with the experimentally accessible reaction volume for the analogous edta system, $\Delta V°_r = -7.9$ cm^3 mol^{-1} (Table S9 A). Although such data treatment should not be overinterpreted, it seems to suggest that water substitution for $[Ni^{II}(tmdta')(H_2O)]^{2-}$ is characterized by a more pronounced dissociative character as compared to $[Ni^{II}(edta')(H_2O)]^{2-}$, which is the expected consequence for the increased shielding on going from the edta to the tmdta ligand.

Despite the complicated mechanistic interpretation for the six-coordinate Ni^{II}−L complexes that arises from the combined water binding/carboxylate dissociation of $[Ni^{II}(L)]^{2-}$ and water dissociation/carboxylate binding processes of $[Ni^{II}(L')(H_2O)]^{2-}$, the findings for the seven-coordinate tmdta complexes allow a precise picture of the structure−reactivity relationship of the complexed metals Fe^{II}, Fe^{III}, and Mn^{II} to be made. The more sterically demanding tmdta ligand requires a pronounced dissociation of the leaving water molecule, which shows the same trend as that for edta but with larger absolute values, e.g., $\Delta V^{‡}$ ($[Fe^{III}(edta)(H_2O)]^{-}$) = +1.9 ± 0.3 cm^3 mol^{-1} and $\Delta V^{‡}$ ($[Mn^{II}(edta)(H_2O)]^{2-}$) = +3.4 ± 0.2 cm^3 mol^{-1} compared to $\Delta V^{‡}$ ($[Fe^{III}(tmdta)(H_2O)]^{-}$) = +7.2 ± 2.7 cm^3 mol^{-1} and $\Delta V^{‡}$ ($[Mn^{II}(tmdta)(H_2O)]^{2-}$) = +8.7 ± 0.6 cm^3 mol^{-1}. The principle of microscopic reversibility for these symmetric solvent exchange reactions requires a weaker bonding to the entering water molecule for the tmdta complexes as compared to the edta relatives. The observed values of k_{ex} exactly show this disfavored water attack, viz. k_{ex}(M-tmdta) < k_{ex}(M-edta), except for $[Fe^{II}(tmdta)(H_2O)]^{2-}$. Here, the explanation is also found in the underlying exchange mechanism. The observed activation volume for $[Fe^{II}(tmdta)(H_2O)]^{2-}$ ($\Delta V^{‡}$ = +15.7 ± 1.5 cm^3 mol^{-1}) clearly speaks for a limiting D mechanism, which accounts for the observation that $k_{ex}([Fe^{II}(tmdta)(H_2O)]^{2-}) > k_{ex}([Fe^{II}(edta)(H_2O)]^{2-})$. Within the series, the reactivity again

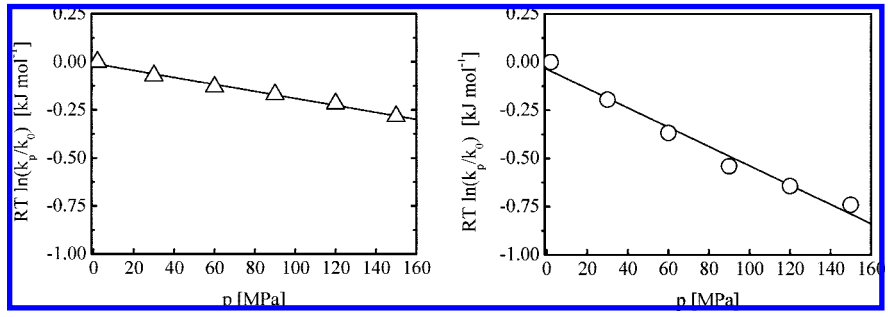

Figure 12. (Left) Pressure dependence of the water substitution rate constant for ring-opened, aqua-pentadentate $[Ni^{II}(edta')(H_2O)]^{2-}$ (Δ with $\Delta V^{‡}_{RO}$ = +1.8 ± 0.1 cm^3 mol^{-1}). The complex concentration at the different pressures was calculated from the known pressure dependence of K, for which $\Delta V°_{reaction}$ = −7.9 ± 0.2 cm^3 mol^{-1} was determined from high-pressure UV−vis measurements (Figure 11). (Right) The pressure dependence of the water substitution rate constant for ring-opened, aqua-pentadentate $[Ni^{II}(tmdta')(H_2O)]^{2-}$ (○ with $\Delta V^{‡}_{RO}$ = +5.0 ± 0.6 cm^3 mol^{-1}) was estimated by applying the reaction volume of the edta complex (Table S9 A, Supporting Information; for further details see text).

Scheme 4. Representative Volume Profiles for the Studied Water Substitution Reactions[a]

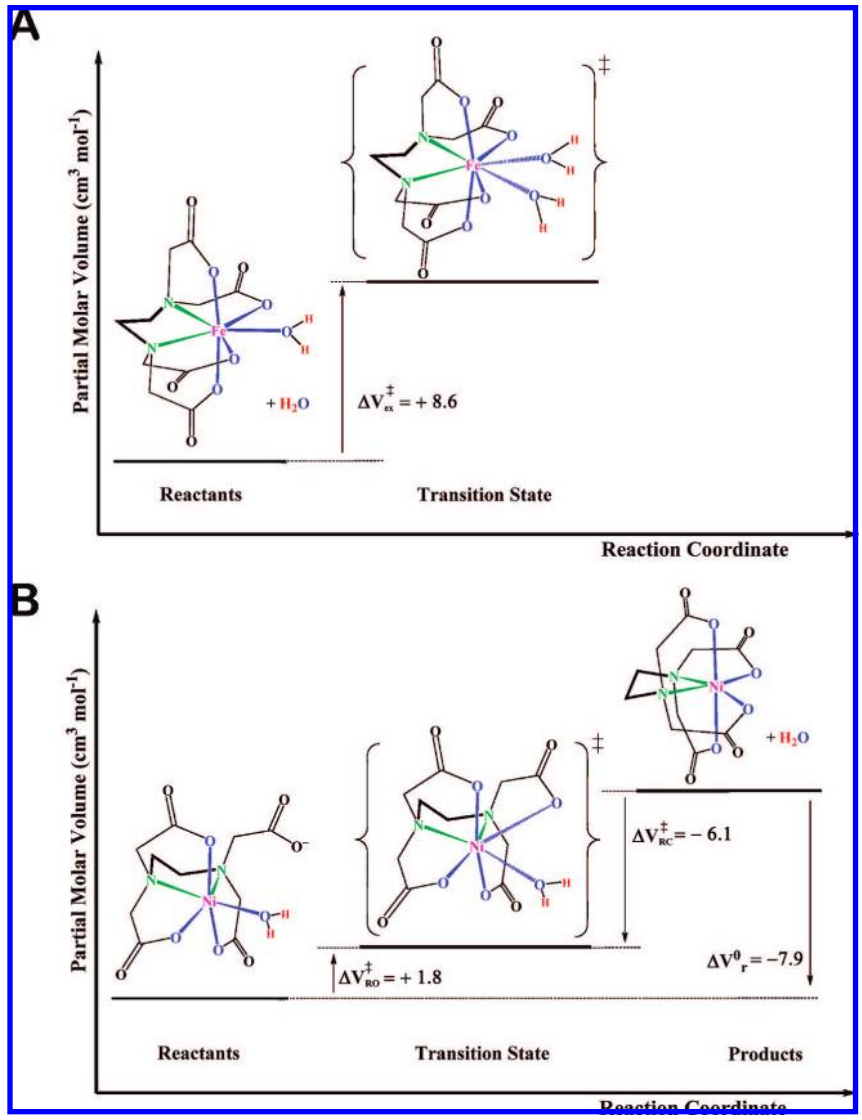

[a] Seven-coordinate species with hexadentate chelate ligands, e.g., $[Fe^{II}(edta)(H_2O)]^{2-}$ (A), exchange water molecules via a pronounced dissociation of the leaving water molecule in the transition state due to the considerable shielding of the metal center. For the equilibrating species $[Ni^{II}(edta)]^{2-}$ and $[Ni^{II}(edta')(H_2O)]^{2-}$ (B), the experimental results revealed a concerted carboxylate binding/water dissociation process for the ring-opened, aqua-pentadentate form, $[Ni^{II}(edta')(H_2O)]^{2-}$ with $\Delta V^{\neq}_{RO} = +1.8 \pm 0.1$ cm^3 mol^{-1}, and $\Delta V^{\neq}_{RC} = -6.1 \pm 0.1$ cm^3 mol^{-1} for the water binding/carboxylate dissociation process of the ring-closed complex species, $[Ni^{II}(edta)]^{2-}$.

increases along the series $[Fe^{II}(tmdta)(H_2O)]^{2-} < [Fe^{III}(tmdta)(H_2O)]^{-} < [Mn^{II}(tmdta)(H_2O)]^{2-}$.

Thus the value of the presented approach lies in the fact that a careful analysis of steric constraints around the metal center is suitable to explain not only the mechanistic details of the exchange process but also the kinetics. In general, we can conclude for seven-coordinate species that the more effective the shielding of the metal center, the more pronounced the dissociative nature of the water substitution process and the smaller the k_{ex} for a given metal center.

Conclusions

The water-exchange kinetics of edta and tmdta complexes of the investigated divalent metal centers are controlled by the d-orbital occupancy. The observed reactivity, $Fe^{II}-L < Mn^{II}-L$, reflects the significant contribution of the LFAE for the exchange kinetics. The rate of water exchange at the trivalent iron complex $[Fe^{III}(edta)(H_2O)]^{-}$ is slower than that for $[Mn^{II}(edta)(H_2O)]^{2-}$, with an isoelectronic configuration, due to the higher charge density of the trivalent species. However, compared to the corresponding fully aquated species, complexation by edta and tmdta ligands leads to an enhanced reactivity in all cases of metal centers with symmetric electronic distribution (viz. Fe^{III} and Mn^{II}). A decreased or comparable reactivity was found for systems with an appreciable angular dependence for ligand field stabilization (Fe^{II}). For seven-coordinate species, the encapsulation of the metal center by the aminopolycarboxylate ligand requires considerable dissociation of the leaving water molecule in the transition state as a result of the meaningful steric shielding of the metal center. The more effective shielding in tmdta complexes compared to their edta relatives leads to significantly larger values for the activation volumes and smaller k_{ex} values. The activation volume found for water exchange on

(72) The authors kindly thank a reviewer for drawing our attention to this fact.

$[Fe^{II}(tmdta)(H_2O)]^{2-}$ speaks for a limiting D mechanism, which can account for the observation that $k_{ex}([Fe^{II}(tmdta)(H_2O)]^{2-}) > k_{ex}([Fe^{II}(edta)(H_2O)]^{2-})$.

The unexpected kinetic behavior found for $[Ni^{II}(edta')(H_2O)]^{2-}$ and $[Ni^{II}(tmdta')(H_2O)]^{2-}$ results from a different coordination number for these complexes. The strong preference for an octahedral coordination environment leads to an observable coordination equilibrium between hexadentate $\rightleftharpoons$ aquapentadentate species in solution. The ring-opened, aquapentadentate form is favored by increasing pressure and decreasing temperature. The kinetic and mechanistic observations for water substitution on $[Ni^{II}(edta')(H_2O)]^{2-}$ are interpreted in terms of concerted water-dissociation/carboxylate-binding processes, which is supported by a largely negative activation entropy and especially the similar rate for ring opening of the edta skeleton (3×10^5 s^{-1}) and for water exchange on $[Ni(edta')(H_2O)]^{2-}$, viz. $(2.6 \pm 0.2) \times 10^5$ s^{-1}, as was already discussed by Evilia.[36] This observation may indicate that the fluxional nature of the edta ligand in an overwhelming number of its complexes[73,74] is driven by fast solvent exchange processes. This conclusion has nicely been confirmed in a ^1H and ^{13}C NMR study of $[Al(edta)]^-$ where the original fluxionality of the ligand in D_2O was completely suppressed in dimethyl sulfoxide-d_6.[74]

The relationship between changes in the ligand architecture and the observed water exchange mechanism could be correlated in a straightforward manner. It is remarkable that, even compared to the reported activation volumes for the corresponding fully aquated metal cations (except Ni^{2+}_{aq}), the mechanism seems to be exclusively controlled by steric hindrance caused by the chelate ligand. On the other hand, the observed reactivity patterns are also a consequence of the d-orbital occupancy, the charge of the central ions, and the nature of the intimate exchange mechanism. The mechanistic features that have been analyzed for the various water exchange processes account for the observed trend in the kinetics, e.g., k_{ex}(M-tmdta) < k_{ex}(M-edta). The unexpected kinetic behavior of the Ni^{II} complexes and of $[Fe^{II}(tmdta)(H_2O)]^{2-}$ could undoubtedly be identified to arise from different mechanisms that operate for the water displacement reaction.

Acknowledgment. The authors gratefully acknowledge financial support from the Deutsche Forschungsgemeinschaft as part of SFB 583 "Redox-active Metal Complexes". R.M. is grateful to the Deutsche Forschungsgemeinschaft for support within the framework of Project ME 1148/7-1.

Supporting Information Available: ^{17}O NMR data for the studied water exchange reactions as a function of temperature and pressure, and spectral data for the determination of K for reaction (7) as a function of pressure. This material is available free of charge via the Internet at http://pubs.acs.org.

JA802842Q

(73) Howarth, O. W.; Moore, P.; Winterton, N. *J. Chem. Soc., Dalton Trans.* **1974**, *2271*, 2276.
(74) Jung, W.-S.; Chung, Y. K.; Shin, D. M.; Kim, S.-D. *Bull. Chem. Soc. Jpn.* **2002**, *75*, 1263–1267.